Study on Electrochemical Effects Assisted Magnetic Abrasive Finishing for Finishing Stainless Steel SUS304

Xu Sun (sunxu8456@126.com)
Special Vehicle Technology Research Center, LongYan University, LongYan, 364000, China
Yongjian Fu
Engineering Research Center of Brittle Materials Machining, HuaQiao University, 361000, China
Wei Lu
Engineering Research Center of Brittle Materials Machining, HuaQiao University, 361000, China
Wei Hang
Key Laboratory E&M, Zhejiang University of Technology, Hangzhou, 310014, China

Research Article

Keywords: electrochemical effect, magnetic abrasive finishing, electrochemical magnetic abrasive finishing, passive films, high machining efficiency

Posted Date: April 26th, 2021

DOI: https://doi.org/10.21203/rs.3.rs-442784/v1

Study on electrochemical effects assisted magnetic abrasive finishing for finishing stainless steel SUS304

Xu Sun[1, 2, 3*], Yongjian Fu[2], Wei Lu[2], Wei Hang[4]

(Email: sunxu8456@126.com; Tel: +86 597 2791925)

[1] Special Vehicle Technology Research Center, LongYan University, LongYan, 364000, China

[2] Engineering Research Center of Brittle Materials Machining, HuaQiao University, 361000, China

[3] Graduate School of Engineering, Utsunomiya University, 7-1-2 Yoto, Utsunomiya, Tochigi, 321-8585, Japan

[4] Key Laboratory E&M, Zhejiang University of Technology, Hangzhou, 310014, China

Abstract

In order to obtain a high accuracy with high machining efficiency for finishing hard alloy metal material, we proposed a hybrid finishing method which is electrochemical (ECM) effects assisted magnetic abrasive finishing (MAF). In this study, the electrochemical magnetic abrasive finishing (EMAF process) was divided into EMAF stage and MAF stage. The metal surface can be easily finished with the passive films formed in electrochemical reactions. Simultaneously, the passive films can be removed by frictional action between magnetic brush and workpiece surface. Thus, the essence of EMAF process is to form and remove the passive films on the workpiece surface. This study focused on investigating the finishing mechanism and finishing characteristics of EMAF process. Through a series of experimental investigations, it can be confirmed that the finishing efficiency is remarkably improved by EMAF process. The optimal experimental result of EMAF process showed that the surface roughness was reduced to less than 30 nm from the original surface roughness 178 nm at 4 min in EMAF stage, and the surface roughness was finally reduced to 20 nm at 10 min in MAF stage. Additionally, we also found the finishing ability of magnetic abrasive decreased after 4 min EMAF stage.

Keyword: electrochemical effect; magnetic abrasive finishing; electrochemical magnetic abrasive finishing; passive films; high machining efficiency

1. Introduction

With the development of semiconductor, optics, biotechnology, aerospace and medical science etc. related technology industries, the demands for surface precision and machining efficiency are becoming higher and higher. In recent years, many new ultra-precision machining technologies have been proposed and applied, in which the magnetic abrasive finishing (MAF) process is proven to be one of effective precision machining methods [1-5]. The quantitative iron particles and quantitative WA abrasive particles are mixed and attracted along the magnetic force lines. The magnetic brush forms on the bottom of the poles. The relative movement between magnetic brush and workpiece surface produce a relative friction on the workpiece surface. Hence, the material removal and mirror-finishing of workpiece surface can be realized by the MAF process.

MAF process has many advantages, such as good flexibility, self-sharpening of magnetic abrasive particles, as well as easy controllability. Especially, MAF process also has penetrating characteristics under the action of magnetic field. Thus, MAF process can be used not only for finishing regular-shaped workpiece [6-8], but also for finishing complex-shaped workpiece [9-11]. MAF process is also suitable for finishing various materials such as resin, glass, ceramics, metal [12-15].

Since the working life of abrasive particles is short, if the abrasive particles can't be promptly replaced, the machining efficiency of MAF process will decrease when MAF process is used to finishing hard alloy metal material or non-metallic materials with high hardness. In order to achieve optimal machining effect, the researchers not only optimized and improved the parameters of magnetic abrasive finishing, but also engaged in the research of combining magnetic abrasive finishing with a variety of processes [16-20]. In these composite processing methods related to magnetic abrasive finishing, electrolytic magnetic abrasive finishing (EMAF) has been proven to be an efficient hybrid finishing method by some researchers. Among them, B.H. Yan proposed using EMAF process to finishing outer surface of tube, the results showed that EMAF with a high electrolytic current has better finishing characteristics than MAF [21]. Zou et al. developed special compound machining tools for EMAF process of plane workpiece and internal tube [22-25]. The electrolytic effects and mechanical finishing can synchronously perform through the compound machining tools in EMAF process [32]. The experimental results showed that not only the higher accuracy surface can be obtained, but also the machining efficiency can be significantly improved by EMAF process. They also respectively investigated the optimal combination of finishing parameters for plane workpiece and internal tube through a series of experiments.

In this study, a hybrid finishing method that electrochemical (ECM) effects assisted magnetic abrasive finishing is proposed. The electrochemical magnetic abrasive finishing (EMAF process) includes two different finishing stages which are the 1st finishing stage (EMAF stage) and the 2nd finishing stage (MAF stage). The high efficiency finishing of workpiece surface is realized in EMAF stage. Then, MAF stage as the 2nd finishing stage plays a role in achieving high precision finishing. According to the research contents of EMAF process, the system model of EMAF process is summarized in Figure 1. Before finishing, the initial values of workpiece surface such as roughness, hardness, undulation, profile accuracy, chemical properties are measured. It can be seen that the combinations of mixed magnetic abrasive, rotational speed of machining tool, feeding speed of X-Y stage, working gap, concentration of electrolyte and working voltage etc. machining influencing factors need to be emphatically investigated in EMAF process. Finally, the surface roughness, undulation and profile accuracy are evaluated. The surface roughness before finishing and after finishing is measured by a contact type roughness meter (Surf-test SV-624-3D, Mitutoyo). The profile accuracy before finishing and after finishing is evaluated through a 3D non-contact optical profiling microscope (Zygo, New View 7300). The surface morphology and residual passive films are observed through a scanning electron microscope (HITACHI S4500). EDX analysis of surface composition is measured by a mini-scope (TM3030Plus).

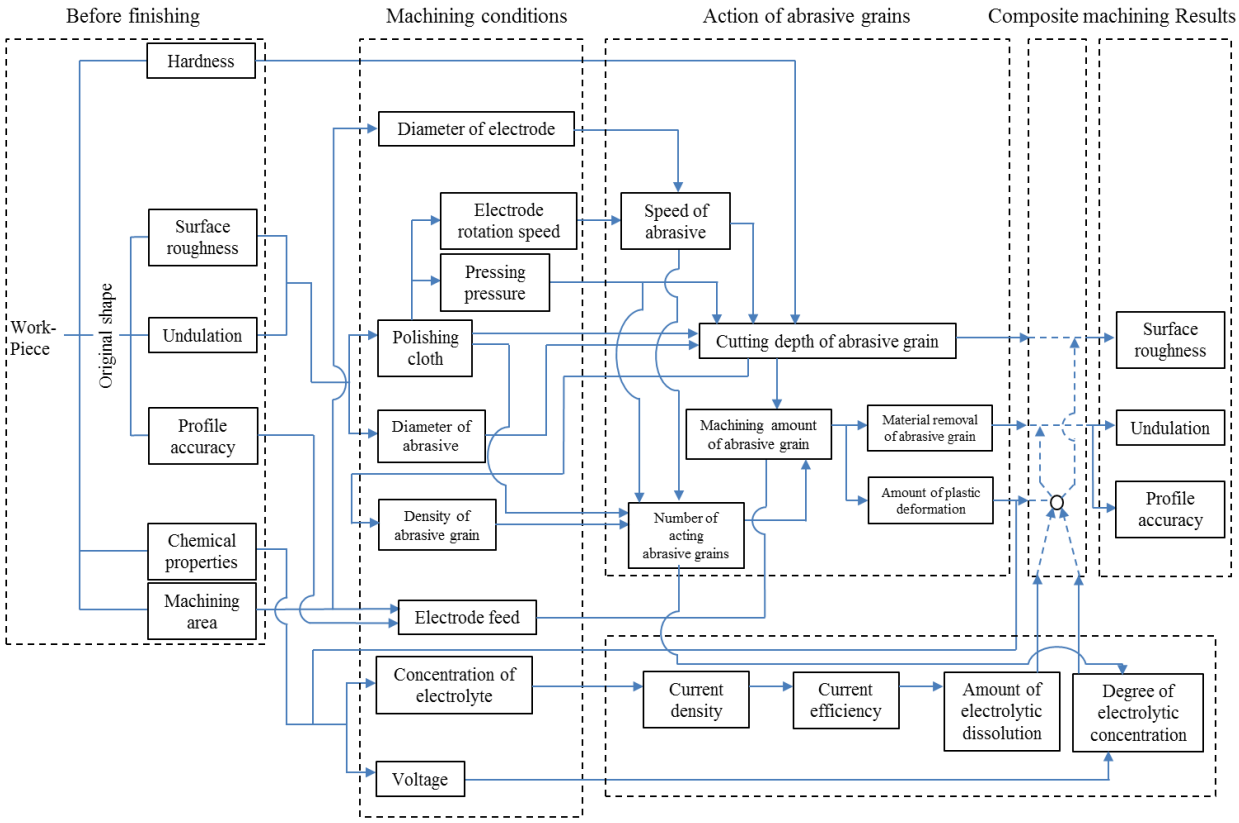

Figure 1 System model of electrochemical magnetic abrasive finishing

2. Experimental procedure

2.1 Basic machining principle of EMAF process

The basic machining principle of EMAF process is shown in Figure 2 (I). Figure 2 (III(a)) shows original surface of workpiece with a lot of protruding portions before finishing. The EMAF stage is shown in Figure 2 (III(b)). The protruding portions of workpiece are preferentially dissolved and the workpiece surface is finitely leveled [26-29]. Moreover, the surface hardness can be also reduced with the passive films form on the workpiece surface by electrochemical effect. Meanwhile, using the magnetic abrasive particles of magnetic brush to exert frictional force on the surface of workpiece, the passive films can be easily and rapidly removed. The high-efficiency machining can be realized in EMAF stage since the hardness of passive films is smaller than the hardness of metal material. Generally, the growth rate of passive films from electrochemical effect is faster than the removal rate of passive films from mechanical action in the hybrid finishing stage. The residual passive films may affect the surface accuracy of workpiece. Hence, MAF process as the final finishing stage is performed after EMAF stage in order to obtain a high-precision surface quality, as shown in Figure 2 (III(c)).

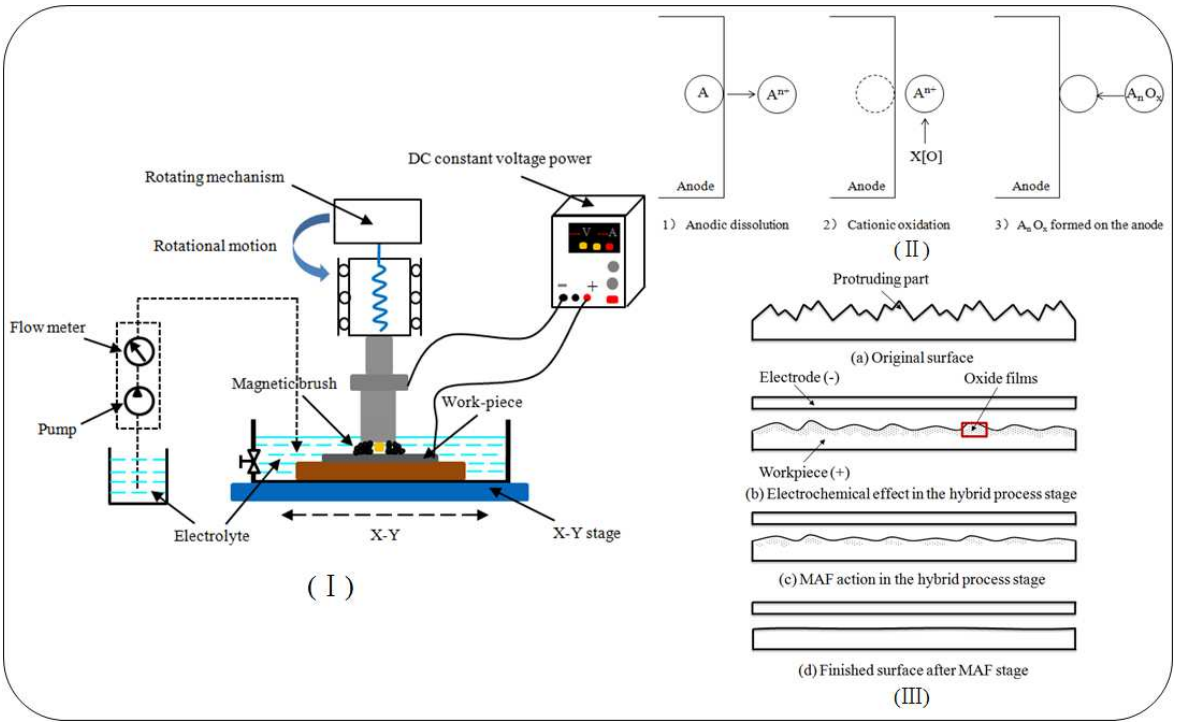

Figure 2 Schematic of EMAF process, (I) the basic machining principle of EMAF process (II) the forming mechanism of passive films in ECM process (III) the whole process that the workpiece is finished by EMAF process

By the way, the forming mechanism of passive films in ECM process as shown in Figure 2 (II) [30]. The $NaNO_3$ solution is adopted as the electrolyte in this study. Under electrochemical effect, electrolyte solution takes place ionization reactions which are shown as Eq. (1) and (2).

$$NaNO_3 \rightarrow Na^+ + NO_3^- \quad (1)$$

$$H_2O \rightarrow H^+ + OH^- \quad (2)$$

Ionization tendency order:

$$Ag^+ > Cu^{2+} > H^+ > Pb^{2+} > Fe^{2+} > Zn^{2+} > Al^{3+} > Mg^{2+} > Na^+ > K^+$$

Discharge ease order: $SO_4^{2-} < NO_3^- < OH^- < Cl^-$

The cations move toward the cathode, anions move toward the anode. According to ionization tendency of cations and discharge ability of anions, the reaction shown as Eq. (3) occurs at the cathode, the reaction shown as Eq. (4) occurs at the anode. Hence, H_2 generate at the cathode and O_2 generate at the anode [31].

$$2H^+ + 2e^- \rightarrow H_2\uparrow \quad (3)$$

$$2OH^- \rightarrow H_2O + 1/2O_2\uparrow + 2e^- \quad (4)$$

The metal ions such as Fe^{3+}, Cr^{6+}, Fe^{2+}, Cr^{3+} and Ni^{2+} etc. elements are eluted by the electrochemical effect on the metal surface [31]. These eluted metal ions are oxidized by the generated O_2 to generate passive films on the workpiece surface.

2.2 Experimental setup

Figure 3 (a) showed the experimental setup of electrochemical magnetic abrasive finishing. The electrochemical magnetic compound machining tool is fixed on the chuck of milling machine. The workpiece as the anode is placed in the container and connects to the positive of DC power. The container is laid on the X-Y stage. The feeding trajectory and feeding velocity of X-Y stage are controlled by the numerical control (NC) program system. The bottom of electrochemical magnetic compound machining tool is shown in Figure 3 (b). In order to synchronously achieve MAF process and electrochemical machining in the EMAF stage, four cylindrical magnetic poles (Nd-Fe-B permanent magnet) and a cross-shape cathode (copper) are embedded in the bottom of electrochemical magnetic compound machining tool. The front of electrochemical magnetic compound machining tool is shown in Figure 3 (c). The electrode connects to copper ring with a wire. To ensure the electrolysis current to be stable, the current flows from the negative pole of DC power to the electrode through a thin copper sheet with elasticity. Additionally, iron particles and WA abrasive are mixed to arrange along the lines of magnetic force to form magnetic brush on the magnetic poles.

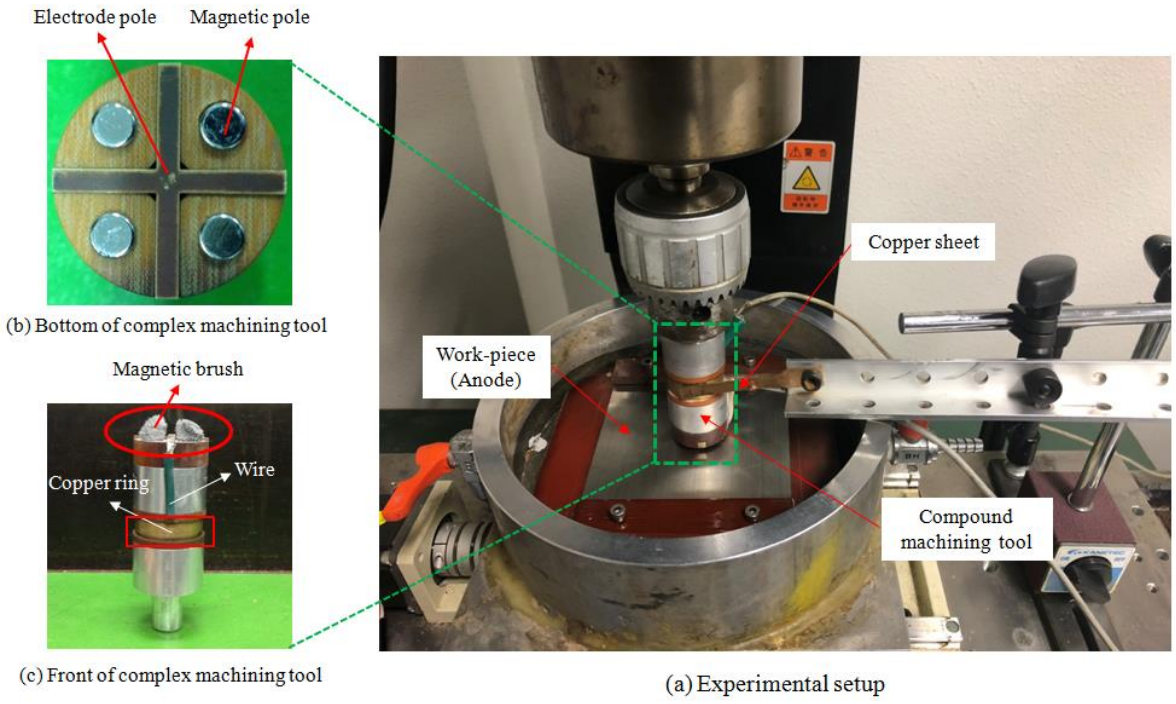

Figure 3 Photo of experimental setup and external views of electrochemical magnetic compound machining tool, (a) experimental setup (b) bottom of complex machining tool (c) front of complex machining tool

2.3 Experimental conditions

2.3.1 Experimental conditions in ECM process

We focused on investigating the influence of working voltage on the surface accuracy. Table 1 showed the detailed experimental conditions of ECM process. The original surface roughness R_a of workpiece was measured at approximate 0.16 ~ 0.2 μm. The working gap was adjusted to 1 mm, the rotational speed of compound machining tool was selected at 450 rpm, and the feeding speed of X-Y stage was adjusted to 5 mm/s. The working voltage was respectively set at 8 V, 10 V and 12 V. The electrolyte concentration was selected as 20 wt%. The finishing time of ECM process was selected at 4 min.

Table 1 Experimental conditions of ECM process

Workpiece	SUS304 plate (100×100×1 mm)
Original roughness R_a	0.16 ~ 0.2 μm
Working gap	1 mm
Feeding speed of stage	5 mm/s
Rotational speed of tool	450 rpm
Working voltage	8 V, 10 V, 12 V
Electrolyte concentration	20 wt%
Finishing time of ECM	4 min

2.3.2 Experimental conditions of EMAF process

According to the experimental investigations of ECM process and the previous report [32], the finishing parameters of EMAF process were determined and shown in Table 2. The total finishing time of EMAF process was selected at 30 min. We focused on investigating the combinations of the EMAF stage time and MAF stage time in order to obtain optimal finishing effect in the shortest time. The finishing time of EMAF stage was respectively 2, 4, 6, 8 and 10 min. The roughness of finished surface was respectively measured after EMAF stage, each 10 min MAF stage and remaining time of MAF stage.

Table 2 Experimental conditions of EMAF process

Workpiece	SUS304 plane (100×100×1 mm)
Original roughness R_a	0.16 ~ 0.2 μm
Mixed magnetic abrasive	Electrolytic iron powder: 149μm
	WA particles: #8000
	Oily grinding fluid
Working gap	1 mm
Feeding speed of stage	5 mm/s
Rotational speed of tool	450 rpm
Working voltage	12 V
Electrolyte concentration	20 wt%
Finishing time(30 min)	2 min (EMAF stage) + 28 min (MAF stage) 4 min (EMAF stage) + 26 min (MAF stage) 6 min (EMAF stage) + 24 min (MAF stage) 8 min (EMAF stage) + 22 min (MAF stage) 10 min (EMAF stage) + 20 min (MAF stage)

2.4 Measurement methods

After each finishing stage, the workpiece is air-dried and measured removal weight. Then, the surface contact-type surface roughness is used to measure the average surface roughness at these three locations (A, B, C) as shown in Fig.4. In addition, the macroscopic confocal images of finished surface were observed by SEM and 3D non-contact optical profiling microscope to evaluate the surface quality.

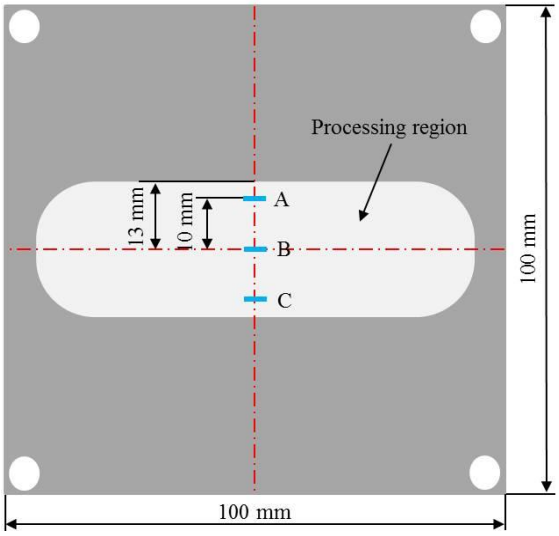

Figure 4 Observed locations of surface specimen

3. Results

3.1 Investigations of electrochemical characteristic in ECM process

3.1.1 Influence of ECM process on surface roughness and material removal

Figure 5 showed the change in surface roughness and material removal under various voltage conditions. Due to the generated heat is too high at 12 V working voltage case, the electrochemical machining can't be performed exceed 6 min. Through quantitatively comparing the change in surface roughness and material removal under various voltage conditions, it was noted that the surface roughness at 12 V working voltage case was remarkably significantly smaller than that under 10 V and 8 V working voltage cases; the material removal at 12 V working voltage case was also significantly more than that under 10 V and 8 V working voltage cases. Thus, it can be regarded that the smaller surface roughness and more material removal can be obtained at relatively higher working voltage condition. We also found that the passive films generated on the finished surface after ECM process. In ECM process, the surface roughness can be limitedly reduced at more than 60nm, but due to the formation of passive films, the mirror-finishing of workpiece surface can't be completed.

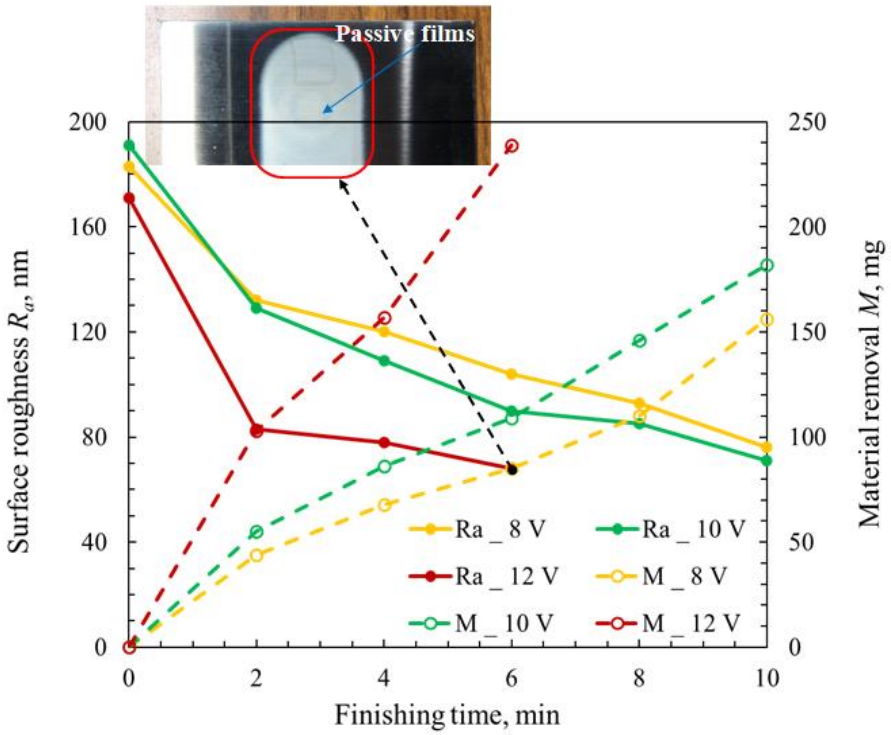

Figure 5 Change in surface roughness R_a and material removal M as a function of electrochemical machining time under various working voltage conditions

3.1.2 Change in surface morphology under different working voltage conditions

The surface morphology was obtained by a scanning electron microscope (SEM), which was shown in Figure 6. It can be seen that these were only initial texture lines on the workpiece surface before ECM process through Figure 6 (a). A lot of micro-pits generated on the workpiece surface, and some unfinished region was found under the condition of 8V working voltage. The size of micro-pits became bigger and the unfinished region became smaller under the condition of 10V working voltage. The maximum diameter of pit (d_{max}= 20 μm) under the condition of 10V working voltage was nearly 3 times of the maximum diameter of pit (d_{max}= 7.5 μm) under the condition of 8V working voltage. The area of pits further expanded and almost the whole surface was machined with varying degrees under the condition of 12V working voltage. Moreover, the depth of micro-porous also became deepen with the working voltage increased.

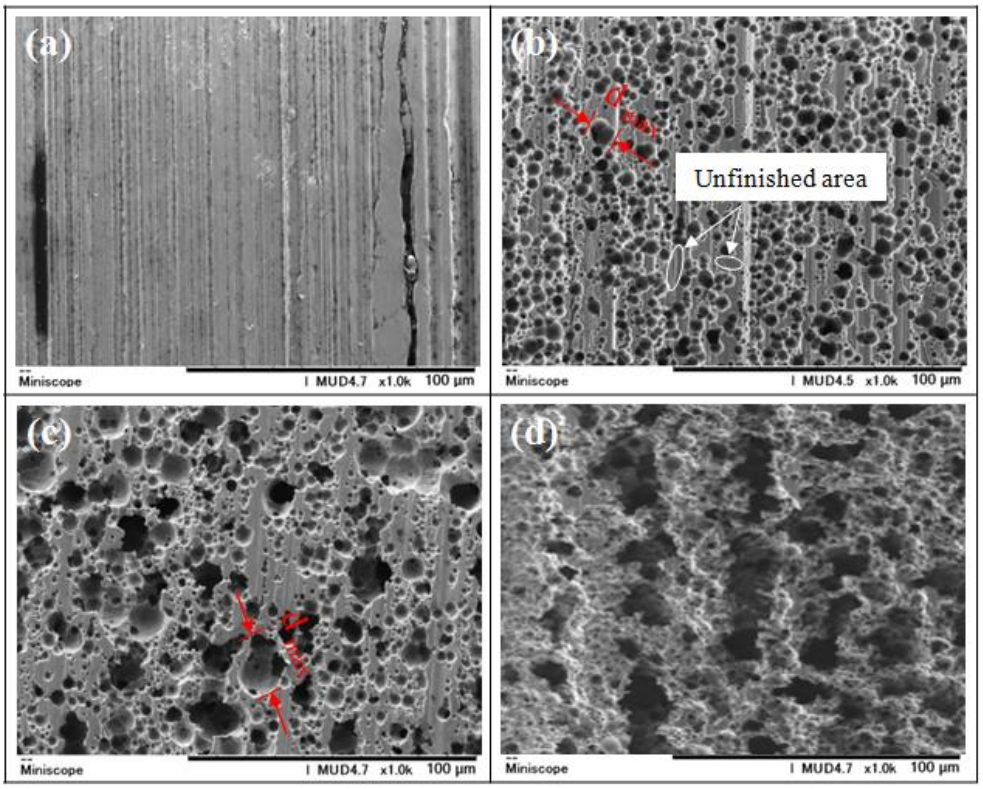

Figure 6 SEM images were obtained under different working voltage conditions in 4 min ECM process. (a) original workpiece surface; (b) under the condition of 8V working voltage; (c) under the condition of 10V working voltage; (c) under the condition of 12V working voltage.

3.1.3 Analysis of EDS and chemical mapping

Finally, we also respectively measured elemental ingredients of workpiece surface before and after ECM process by a mini-scope. The elemental ingredients of original surface were shown in Figure 7 (a). Figure 7 (b), (c) and (d) respectively showed that the elemental ingredients of finished surface after ECM process under different working voltage conditions. The measured results proved that the content of "Fe", "Cr" elements after ECM process was less than the elemental content of original surface. Moreover, the content of "Fe", "Cr" elements also decreased with the working voltage increased. The metal cations dissolved out from SUS304 workpiece surface under the electrochemical effect. Hence, the content of "Fe", "Cr" elements decreased after ECM process. According to Faraday law, the dissolved amount of metal cations can be quantitatively calculated by the formula (5).

$$W = (I \cdot t/96500)\ (M/n) \tag{5}$$

Where, "W" is elution amount, "I" is electrolysis current, "M" is atomic weight, "n" is atomic valence. The dissolved amount of metal ions is proportional to electrolysis current and machining time. Thereby, "Fe", "Cr" elements of workpiece surface dissolved more at higher working voltage.

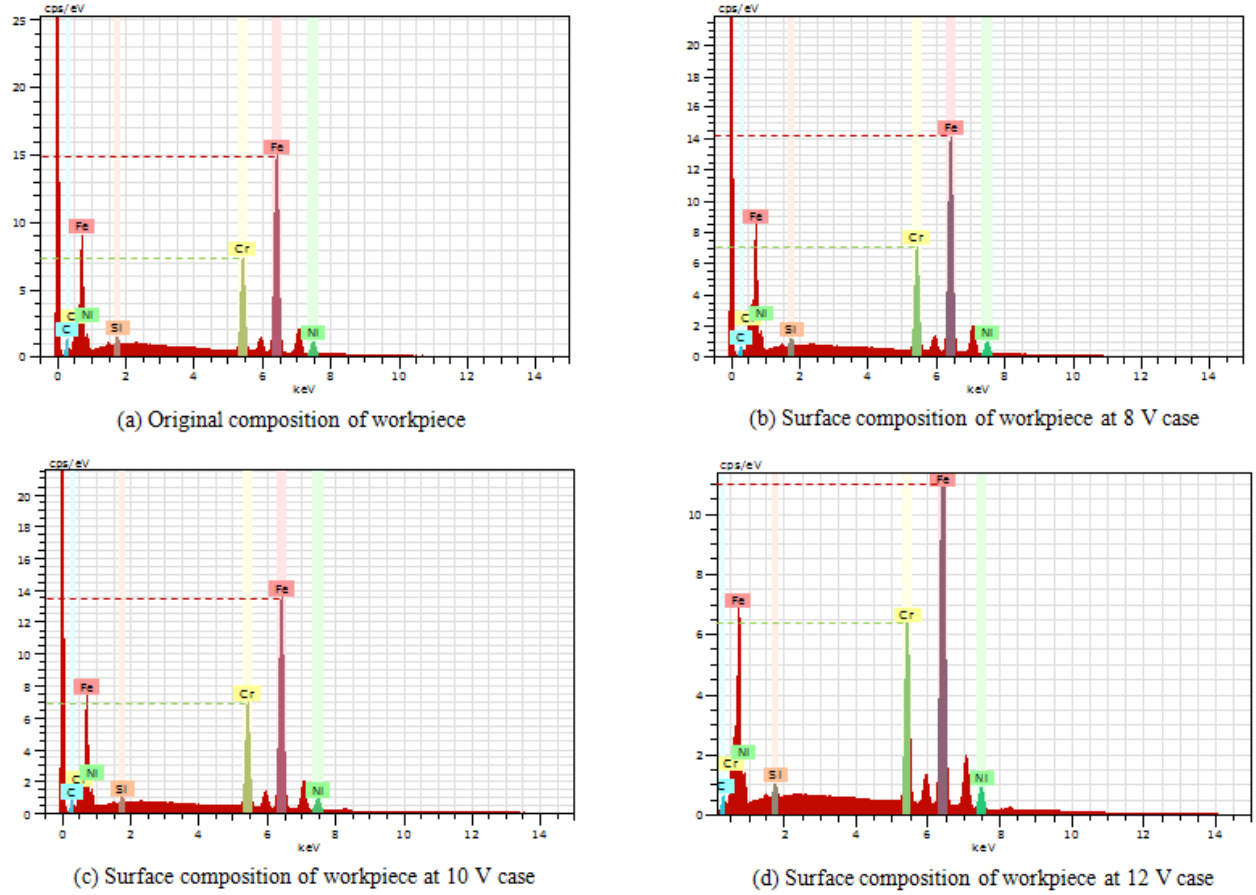

Figure 7 EDS of original surface and finished surface at different working voltage cases

Since the major composition of SUS304 material is constituted by Fe (70%), Cr (20%), Ni (10%) elements, Figure 8 described the chemical mappings of these three representative elements under various working voltage conditions. Fe, Cr, Ni elements were respectively represented by red, yellow and green. The color of these three elements was unitary and evenly distributed before ECM process. The black dots which were substances with unknown elements formed on the measured region and the distributions of these three elements were non-uniform after ECM process. Additionally, the quantity and size of black dots increased with the working voltage increased. The measuring results revealed that the content of each element decreased with the unknown elements increased since the original color area of each element decreased in ECM process. It was also seen that the brightness of these three elements dimmed with the working voltage increased. It was considered that the metal elements began completely to dissolve from workpiece surface and the elution amount of metal elements was the most under 12 V working voltage case.

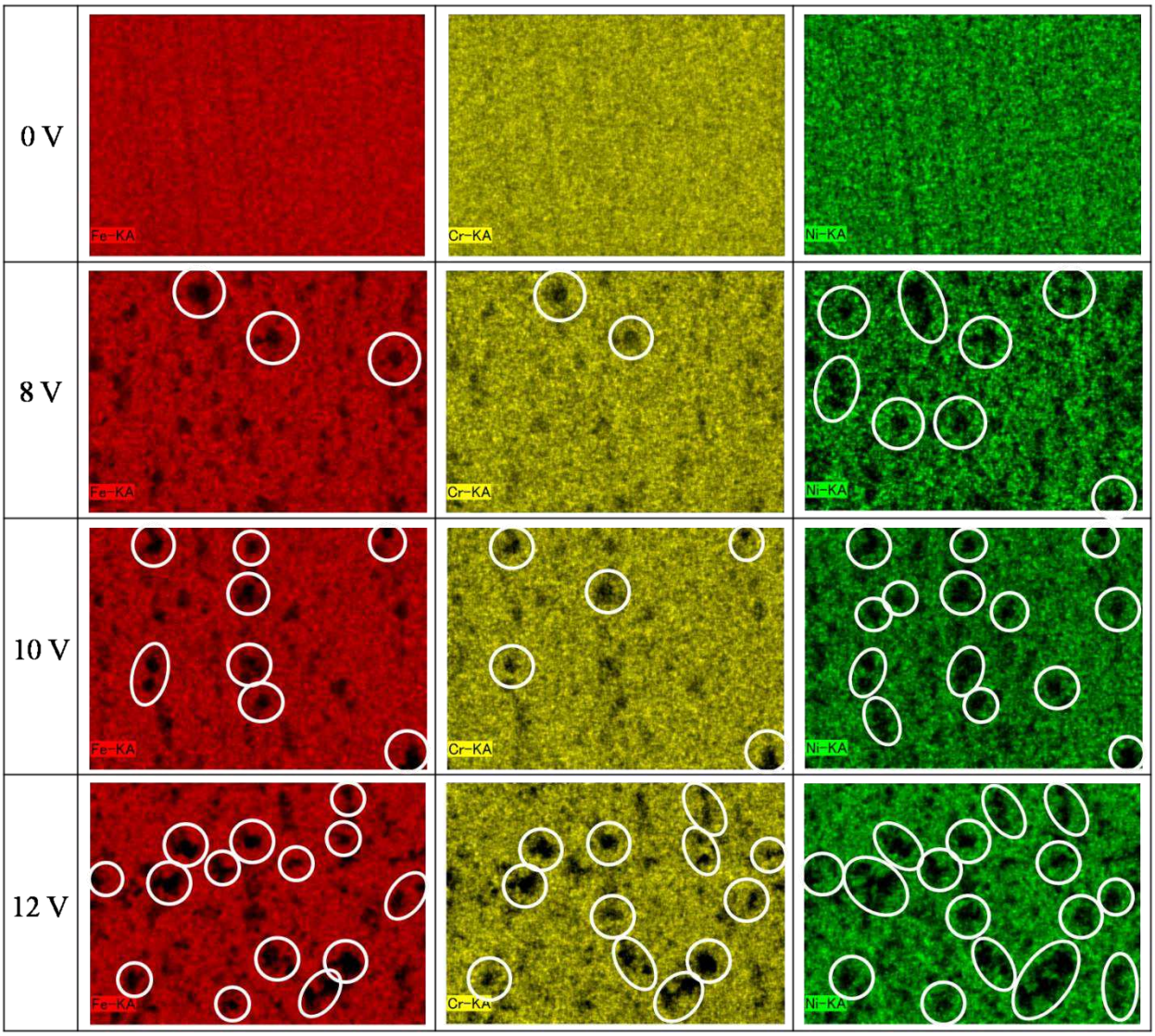

Figure 8 Chemical mapping of Fe, Cr and Ni elements after ECM process under various working voltage conditions

3.1.4 Influence of working voltage on the hardness of workpiece surface

Finally, we compared the surface hardness before and after ECM process. From Figure 9, it can be clearly found that the hardness HV of finished surface decreased with the passive films generated on the workpiece surface under the electrochemical effect. Moreover, the hardness of finished surface decreased with the increase of machining time and working voltage. The hardness (HV) of finished surface can be maximally reduced from 308 HRC to 262 HRC under the condition of 12 V working voltage at 6 min machining time. The hardness (HV) of workpiece surface was maximally reduced by 15% with the passive films formed on the workpiece surface. Thence, it can be considered the better ECM processing characteristics of working voltage can be obtained at 12 V working voltage case.

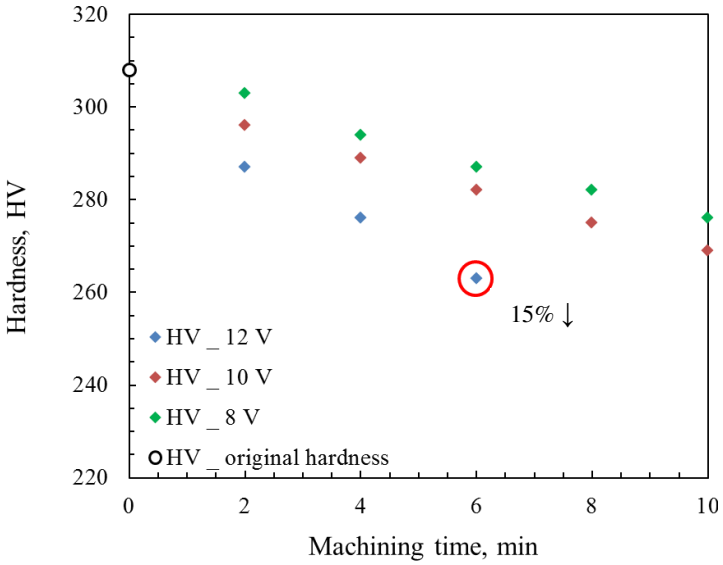

Figure 9 Change in hardness of workpiece surface under the electrochemical effect

3.2 Experimental results of EMAF process

The experiments of EMAF stage were firstly performed before researching the EMAF process. Figure 10 showed the change in surface roughness and material removal as a function in EMAF stage under the conditions of different working voltage and finishing time. It can be seen that the surface roughness significantly decreased under the condition of 12 V working voltage. The mix surface roughness occurred at 4 min under the condition of 12 V working voltage. Then the surface roughness slightly increased after 4 min. As the passive films accumulated on the workpiece surface, the material removal rate before 4 min was remarkably more than that after 4 min under the condition of 12 V working voltage.

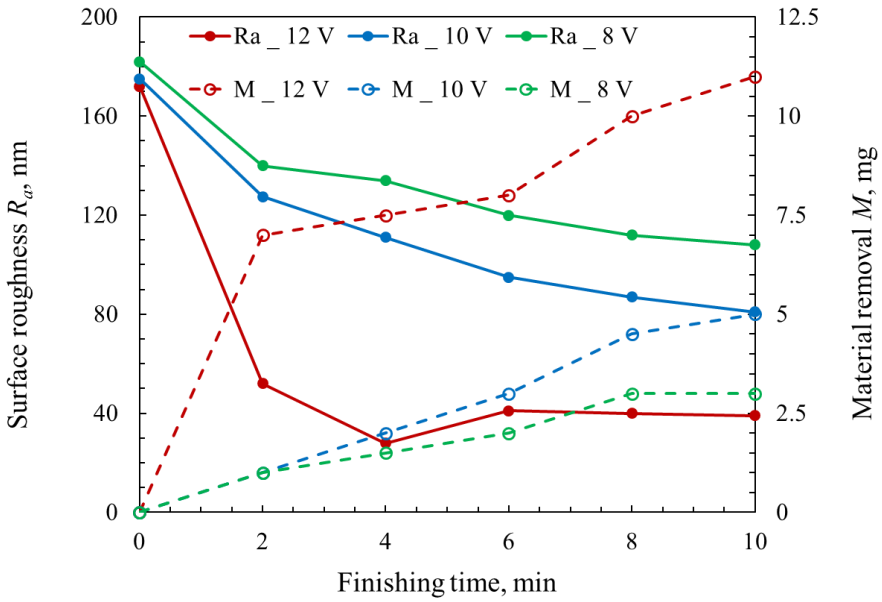

Figure 10 Change in surface roughness R_a and material removal M as a function under the conditions of different working voltage and finishing time

Figure 11 showed the change in surface roughness and material removal as a function under the different combination conditions of EMAF stage time and MAF stage time. Through comparing the experimental results, it can be noted that the surface roughness drastically decreased in EMAF stage, the material removal in EMAF stage was obviously more than that in MAF stage. The material removal was approximately 7 ~ 10 mg in EMAF stage, and that was approximately 4 ~ 6 mg in MAF stage. The material removal rate in EMAF stage was nearly 7 times than that in MAF stage. Furthermore, the optimal experimental result of EMAF process showed that the surface roughness was reduced to less than 30 nm at 4 min EMAF stage. Then, it was reduced to 20 nm at 10 min MAF stage. However, the surface roughness almost didn't change after 10 min MAF stage. In other words, the optimal surface accuracy can be obtained at 14 min EMAF process under the combination condition of 4 min EMAF stage combined with 26 min MAF stage. As the electrochemical effect was not enough in 2 min EMAF stage, and the electrochemical effect was excessive in 6 min, 8 min and 10 min EMAF stage.

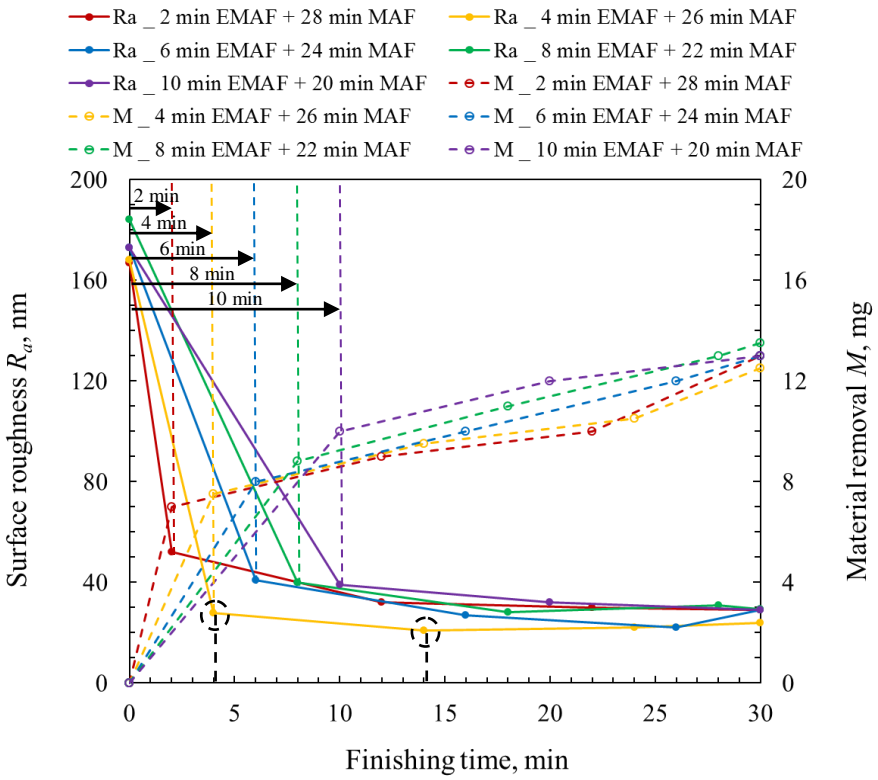

Figure 11 Change in surface roughness R_a and material removal M as a function under the different combination conditions of EMAF stage time and MAF stage time

The 3D morphology of original workpiece surface and finished surface after various finishing stages was shown in Figure 12. It was seen that the protruding part of original surface was rapidly removed after EMAF stage, as shown in Figure 12 (b). However, some deep concave hairlines still remained on the finished surface after EMAF stage. Finally, it can be found that the residual concave hairlines were almost completely eliminated after MAF stage through the obtained 3D morphology of Figure 12 (c). At this moment, only the

number of finishing traces was seen on the finished surface. Thus, the MAF stage plays a vital role in improving the surface accuracy in EMAF process.

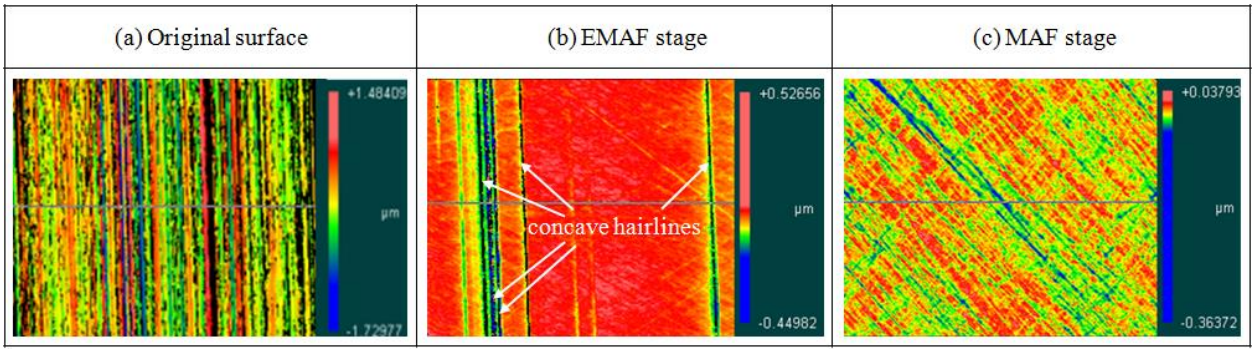

Figure 12 3D morphology of unfinished surface and finished surface after two different finishing stages

Figure 13 showed the macroscopic confocal images of finished surface after EMAF stage and MAF stage. Figure 13 (a) showed the SEM photograph of finished surface after 4 min EMAF stage. A small amount of micro-porous and finishing traces were clearly seen on the finished surface after EMAF stage. It indicated that the action of mechanical machining can't completely remove the generated passive films from electrochemical effect in EMAF stage. The SEM photograph of finished surface after 26 min MAF stage was shown in Figure 13 (b). The residual passive films were completely removed after MAF stage. Hence, it can be confirmed that MAF stage plays an essential role to achieve precision machining in EMAF process.

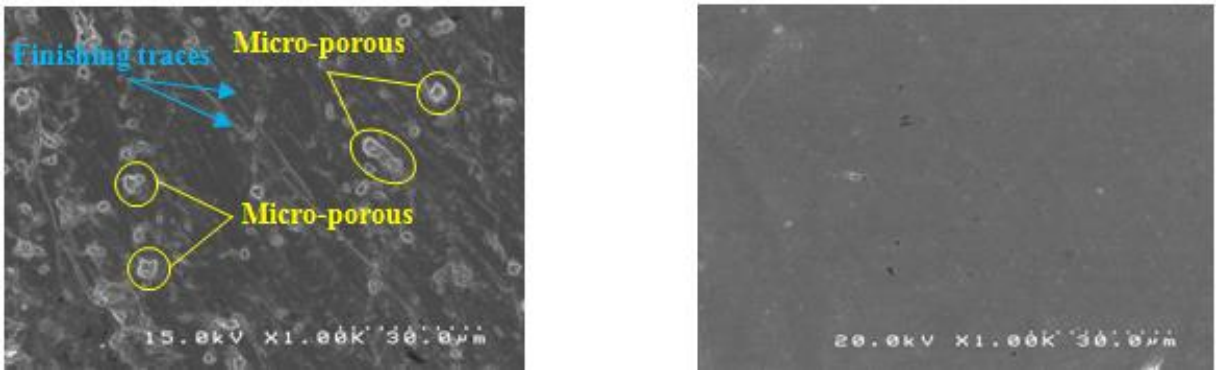

(a) After 4 min EMAF stage (b) After 26 min MAF stage

Figure 13 Macroscopic confocal images of finished surface after EMAF stage and MAF stage

4. Discussions

4.1 Different of electrochemical effect in ECM process and EMAF stage

In ECM process, the deposits and gas were generated in the electrolyte with the electrochemical reaction occurred. The deposits appeared dark green in the early stage of ECM process, the color of deposits deepened with the machining time increased. Finally, the generated deposits turned brown as shown in Figure 14 (a). Fe,

Cr and Ni etc. metal cations dissolved out from workpiece surface by the electrochemical effect. With the generated O_2, Fe^{x+} from divalent ion was oxidized to trivalent ion, Cr^{x+} from trivalent ion changed to hexavalent ion. The dissolved metal cations reacted with the free OH^- to generate the deposits, as shown in formula (6) ~ (11).

$$Fe^{2+} + 2OH^- \rightarrow Fe(OH)_2 \downarrow \text{(dark green)} \quad (6)$$

$$Fe^{3+} + 3OH^- \rightarrow Fe(OH)_3 \downarrow \text{(brown)} \quad (7)$$

$$4Fe(OH)_2 + 2H_2O + O_2 \rightarrow 4Fe(OH)_3 \downarrow \quad (8)$$

$$Cr^{3+} + 3OH^- \rightarrow Cr(OH)_3 \downarrow \quad (9)$$

$$Cr^{3+} + 3OH^- \rightarrow Cr(OH)_3 \downarrow \quad (10)$$

$$Ni^{2+} + 2OH^- \rightarrow Ni(OH)_2 \downarrow \quad (11)$$

From Figure 14 (b), it was seen that the workpiece surface was covered by the mixed magnetic abrasive slurry in EMAF stage, and the electrochemical reaction weakly occurred without the gas and the brown deposits generated in EMAF stage, which compared with single ECM process. It maybe the mixed magnetic abrasive slurry hindered the conduction of electrolysis current.

(a) Workpiece sample in ECM process (b) Workpiece sample in EMAF stage

Figure 14 The SUS304 workpiece was machined in ECM process and EMAF stage

4.2 Different of electrolysis current in ECM process and EMAF stage

In order to explore the reason for the weakening of the electrochemical reaction in EMAF stage, we used the current recorder to measure separately electrolysis current in EMAF stage and ECM process, which was shown in Figure 15. When the working voltage was 12 V, it was seen that the amplitude of electrolysis current in ECM process was obviously bigger than that in EMAF stage. The fluctuation of electrolysis current was severe before 45s ECM process, it drastically decreased and tended to stabilize after 45s ECM process. The peak value of electrolysis current reached to 14.6A in ECM process. However, the peak value of electrolysis current

was 3.9A in EMAF stage. The fluctuation of electrolysis current was stable at 1.5 ~ 1.8A from beginning to end. The resistivity ρ of electrolyte became larger in EMAF stage since the workpiece surface was covered by the abrasive slurry. The conductivity σ can be calculated by the Eq. (12).

$$\sigma = 1/\rho \tag{12}$$

Through the Eq. (12), it was known that the conductivity σ and resistivity ρ were inversely proportional. Thus, the conductivity σ was smaller in EMAF stage than that in ECM process. Due to the difference of electrolysis current in EMAF stage and ECM process, the degree of electrochemical reaction was different in these two processes.

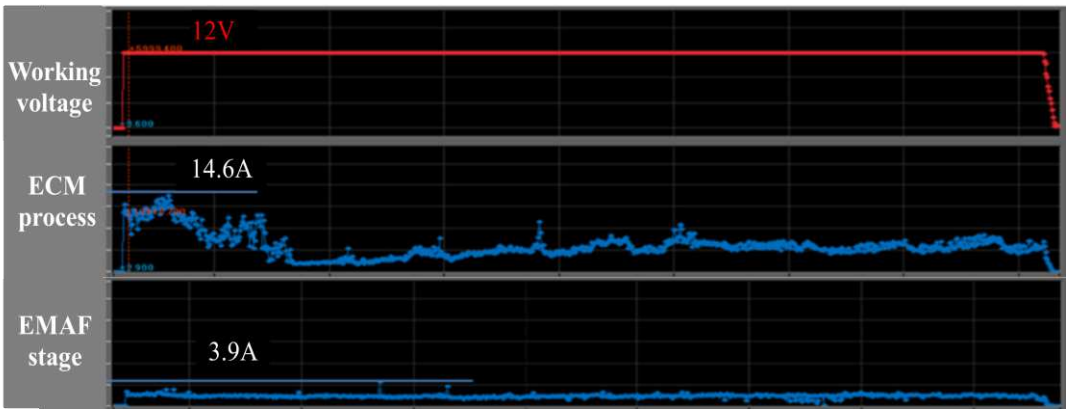

Figure 15 Electrolysis current in two different processing

4.3 Mechanical behavior of magnetic abrasive in EMAF stage

Figure 16 showed the photographs of the unfinished surface and the finished surface with three different finishing methods which were respectively traditional MAF process, ECM process and EMAF process. It can be seen that the mirror effect of finished surface by ECM process was not well. Although the surface roughness can rapidly reach to below 100 nm in ECM process, the brightness of finished surface was not well since the passive films formed on the finished surface. Additionally, it was also regarded that the mirror finishing can be achieved by both traditional MAF process and EMAF process.

Though both traditional MAF process and EMAF process can achieve nano-scale mirror finished, the effective finishing area was approximately 90 × 30 mm^2 in MAF process and 80 × 24 mm^2 in EMAF process. The effective finishing area in EMAF process was about 70% of the effective finishing area in MAF process.

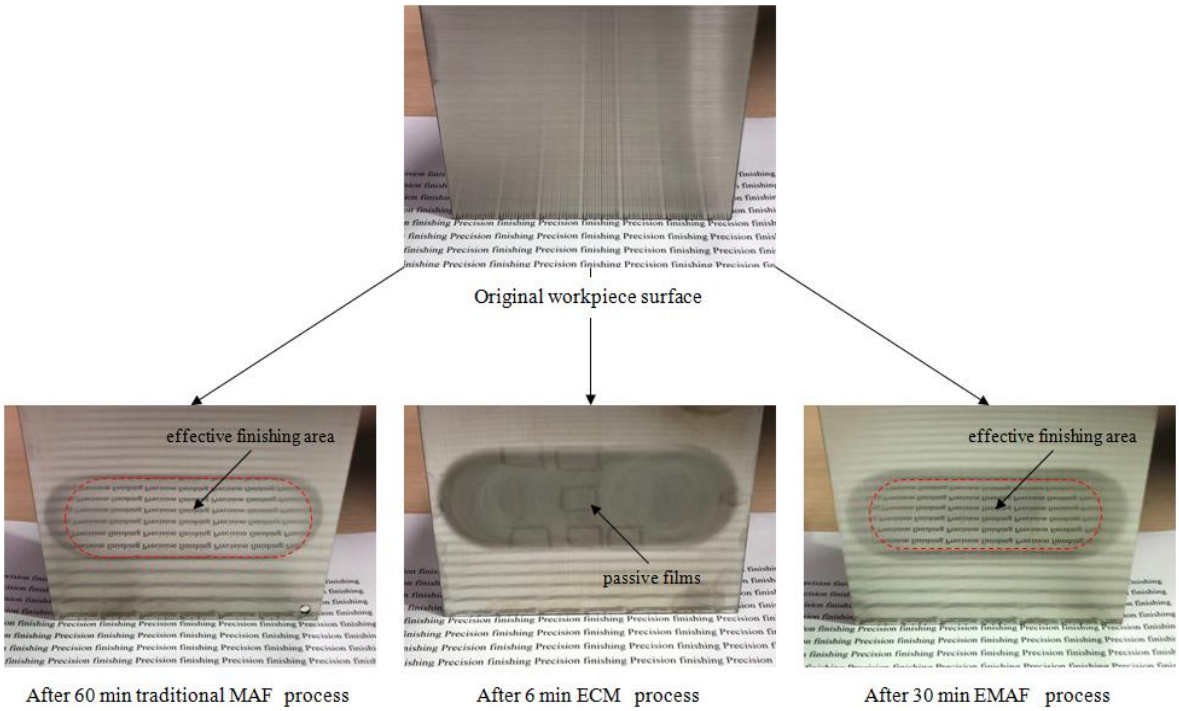

Figure 16 Photographs of unfinished surface and finished surface with three different finishing methods

Figure 17 showed the SEM images of change in mixed magnetic abrasive under the different conditions of EMAF stage time and working voltage. It can be considered that the size of mixed magnetic abrasive drastically decreased with EMAF stage time increased at the same working voltage case; the size of mixed magnetic abrasive slightly decreased with working voltage increased at the same EMAF stage time case. The iron powder of mixed magnetic abrasive was consumed by the electrochemical effect in EMAF stage. The WA abrasive which attached to the iron powder was also lost with the iron powder was consumed. Thus, the effective finishing area in EMAF process was smaller than that in MAF process.

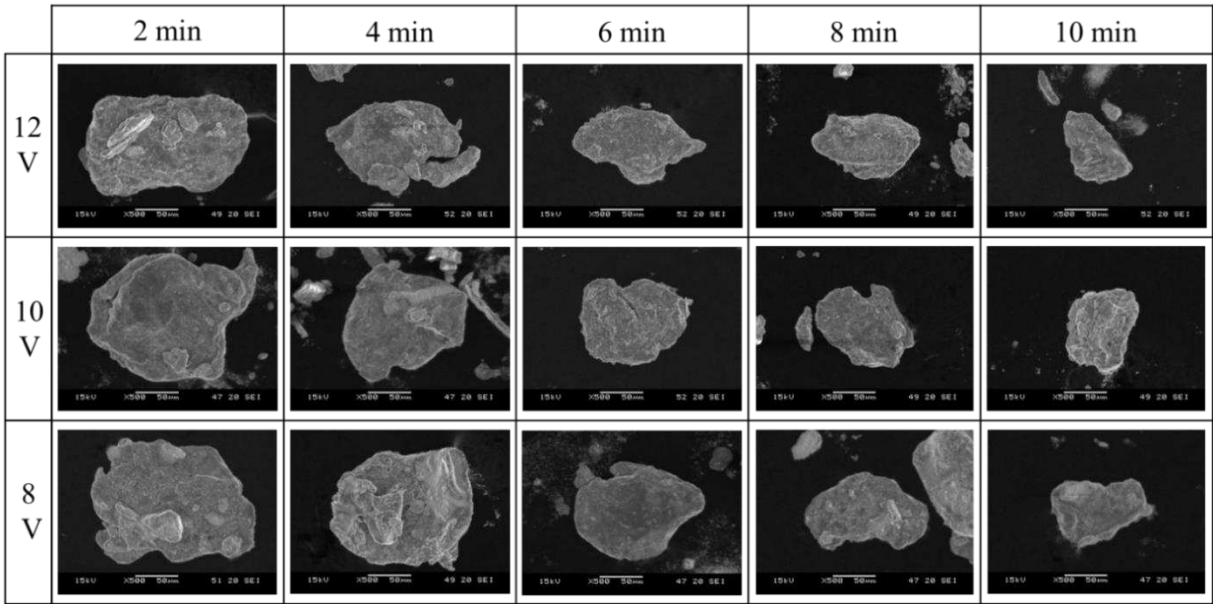

Figure 17 SEM images of change in mixed magnetic abrasive under the different conditions of EMAF stage time and working voltage

Furthermore, according to the aforementioned SEM images in ECM process from Figure 6 and change in size of mixed magnetic abrasive in EMAF stage from Figure 17, it was easy to understand why the optimal surface accuracy can be obtained under the combination condition of 4 min EMAF stage and 26 min MAF stage. Since the electrochemical effect was not enough in 2 min EMAF stage and the size of mixed magnetic abrasive drastically decreased in 6 min, 8 min, 10 min EMAF stage (the finishing capacity of mixed magnetic abrasive was almost ignored after 6 min EMAF stage), the finishing efficiency was low in 2 min and 6 min, 8 min, 10 min EMAF stage. However, 4 min EMAF stage was considered as the optimal finishing time for EMAF process. The generated passive films from ECM process can be maximally removed by the mechanical machining in 4 min EMAF stage.

5. Conclusions

This paper proposed a hybrid finishing method which is electrochemical magnetic abrasive finishing (EMAF process) to finishing SUS304 workpiece. The essence of EMAF process is to form and remove the passive films from electrochemical effect. The main conclusions were summarized as follows:

1. The EMAF process includes EMAF stage and MAF stage in this study. The high efficiency finishing is realized in EMAF stage since the passive films form under electrochemical effect. MAF stage as the finally finishing stage plays a role in achieving high precision finishing. The experimental result showed that the surface roughness was reduced to less than 30 nm at 4 min EMAF stage, and it reached to 20 nm at 10 min MAF stage.

2. It was clarified that the passive films generated and the surface hardness was decreased under the electrochemical effect in ECM process. Moreover, the brown deposits generated with the electrochemical reaction occurred in ECM process. It was proved that the content of “Fe”, “Cr” elements on the workpiece surface was measured to decrease after ECM process through the EDS results.

3. After EMAF stage, a small amount of passive films still existed on the finished surface. This is because that the electrochemical effect was stronger than the mechanical action in EMAF stage.

4. As the size of mixed magnetic abrasive drastically decreased in EMAF stage, the effective finishing area in EMAF process was smaller than it in MAF process. Therefore, the larger size in iron powder was considered to use in future research.

5. Compared to the electrolysis current in ECM process, the electrolysis current was obviously lower and stable in EMAF stage. Additionally, the degree of electrochemical effect was very weak in EMAF stage, and there was not obvious deposit generated in electrolyte.

Declarations

Funding: We declared the valuable contributions and support of this study from the Utsunomiya University Creative Department for Innovation (CDI), Longyan University Dr. Start Fund, Huaqiao University

Engineering Research Center of Brittle Materials Machining (MOE, 2020IME-003) and Middle-aged and Young Teachers' Education Research Project of Fujian (JAT190750).

Conflicts of interest: The authors declared that they have no conflict of interest.

Availability of data and material: Not applicable.

Code availability: Not applicable.

Ethics approval: Not applicable.

Consent to participate: Not applicable.

Consent for publication: Not applicable.

Authors' contributions: the corresponding author Xu Sun has been responsible for writing this paper, proposing method, planning experiments, developing experiments and data collation. Yongjian Fu and Wei Lu have been responsible for performing experiments. Wei Hang has been statistically analyzing EDS and measuring working.

Reference

[1] T. Shinmura, K. Takazawa, E. Hatano, M. Matsunaga, Study on Magnetic Abrasive Finishing, [J] CIRP Annals - Manufacturing Technology. 39 (1990) 325-328.

[2] T. Mori, K. Hirota, Y. Kawashima, Clarification of magnetic abrasive finishing mechanism, [J] Journal of Materials Processing Technology. 143 (2003) 682-686.

[3] Analysis of surface texture generated by a flexible magnetic abrasive brush, [J] Wear. 259 (2005) 1254-1261.

[4] Characterization of the Magnetic Abrasive Finishing Method and Its Application to Deburring, [J] Key Engineering Materials. 524 (2005) 291-296.

[5] Effective Deburring of Micro Burr using Magnetic Abrasive Finishing, [J] Journal of the Korean Society for Precision Engineering. 22 (2005) 7-13.

[6] Study of the surface modification resulting from an internal magnetic abrasive finishing process, [J] Wear. 225 (1999) 246-255.

[7] Study on the inner surface finishing of tubing by magnetic abrasive finishing, [J] International Journal of Machine Tools and Manufacture. 45 (2005) 43-49.

[8] AN EXPERIMENTAL ANALYSIS OF MAGNETIC ABRASIVES FINISHING OF PLANE SURFACES, [J] Machining Science and Technology. 10 (2006) 323-340.

[9] Development of an Internal Magnetic Abrasive Finishing Process for Nonferromagnetic Complex Shaped Tubes, [J] International Journal Series C Mechanical Systems, Machine Elements and Manufacturing. 44 (2001) 275-281.

[10] Study of magnetic abrasive finishing in free-form surface operations using the Taguchi method, [J] International Journal of Advanced Manufacturing Technology. 34 (2007) 122-130.

[11] Theoretical Research on Polishing Free-Form Surface with Magnetic Abrasive Finishing, [J] Key Engineering Materials. 760 (2009) 404-408.

[12] Magnetic Field Assisted Finishing of Ceramics—Part III: On the Thermal Aspects of Magnetic Abrasive Finishing (MAF) of Ceramic Rollers, [J] Journal of Tribology. 120 (1998) 660-667.

[13] Optimization in MAF operations using Taguchi parameter design for AISI304 stainless steel, [J] International Journal of Advanced Manufacturing Technology. 42 (2009) 595-605.

[14] Optimization in MAF operations using Taguchi parameter design for AISI304 stainless steel, [J] International Journal of Advanced Manufacturing Technology. 42 (2009) 595-605.

[15] Nano-finishing of BK7 optical glass using magnetic abrasive finishing process, [J] Applied Optics. 54 (2015) 2199-2207.

[16] Vertical vibration-assisted magnetic abrasive finishing and deburring for magnesium alloy, [J] International Journal of Machine Tools and Manufacture. 44 (2004) 1297-1303.

[17] N. Sihag, P. Kala, P. M. Pandey, Experimental investigations of chemo-ultrasonic assisted magnetic abrasive finishing process, [J] International Journal of Precision Technology. 5 (2015) 246-260.

[18] Effects of Horizontal Vibration Assistance on Surface Roughness in Magnetic Abrasive Finishing, [J] Advanced Materials Research. 849 (2009) 246-251.

[19] Ultrasonic assisted magnetic abrasive finishing of hardened AISI 52100 steel using unbonded SiC abrasives, [J] International Journal of Refractory Metals and Hard Materials. 29 (2010) 68-77.

[20] Study on complex micro surface finishing of alumina ceramic by the magnetic abrasive finishing process using alternating magnetic field, [J] International Journal of Advanced Manufacturing Technology. 97 (2018) 2193-2202.

[21] Electrolytic magnetic abrasive finishing, [J] Journal of Machine Tools and Manufacture. 43 (2003) 1355-1366.

[22] X. Sun, Y.H. Zou, Development of magnetic abrasive finishing combined with electrolytic process for finishing SUS304 stainless steel plane, Int. J. Adv. Manuf. Technol. 92 (2017) 3373-3384.

[23] X. Sun, Y.H. Zou, Study on magnetic abrasive finishing combined with electrolytic process, Int. J. Abrasive Technology. 9 (2019) 129-137.

[24] M.M. Ridha, Y.H. Zou, H.S. Sugiyama, Development of a new internal finishing of tube by magnetic abrasive finishing process combined with electrochemical machining, Journal of Mechanical Engineering and Applications. 3 (2015) 22-29.

[25] Y.H. Zou, B.J. Xing, X. Sun, Study on the magnetic abrasive finishing combined with electrolytic process—investigation of machining mechanism, Int J Adv Manuf Technol. 108 (2020) 1675–1689.

[26] Y.O. Kimoto, Ultra-precision machining by electrolytic complex method, Tokyo: aipishi. (1994) 111-116. (in Japanese)

[27] A.M. Kumar, P. Sudhagar, S. Ramakrishna, Y.S. Kang, H. Kim, Z.M. Gasem, N. Rajendran, Evaluation of chemically modified Ti–5Mo–3Fe alloy surface: Electrochemical aspects and in vitro bioactivity on MG63 cells, Applied Surface Scienc. 307 (2014) 52-61.

[28] F.S. Utkua, E. Seckinb, G. Gollerb, C. Tamerlerc, M. Urgen, Electrochemically designed interfaces: Hydroxyapatite coated macro-mesoporous titania surfaces, Applied Surface Science. 350 (2015) 62-68.

[29] H.Z. Zhang, X.G. Shi, A. Tian, L. Wang, C.W. Liu, Electrochemical properties of Ti3+ doped Ag-Ti nanotube arrays coated with hydroxyapatite, Applied Surface Science. 436 (2018) 579-584.

[30] V. Kamakoti, N.R. Shanmugam, A.S. Tanak, B. Jagannath, S. Prasad, Investigation of molybdenum-crosslinker interfaces for affinity based electrochemical biosensing applications, Applied Surface Science. 436 (2018) 441-450.

[31] K.N. Fan, Z.J. Jin, J. Guo, Z.B. Wang, G.N. Jiang, Investigation on the surface layer formed during electrochemical modification of pure iron, Applied Surface Science. 466 (2019) 466-471.

[32] X. Sun, Y.H. Zou, Study on electrolytic magnetic abrasive finishing stainless steel sus304 plane with a special compound machining tool, Journal of Manufacturing and Materials Processing. 2 (2018) 41–53.

Figures

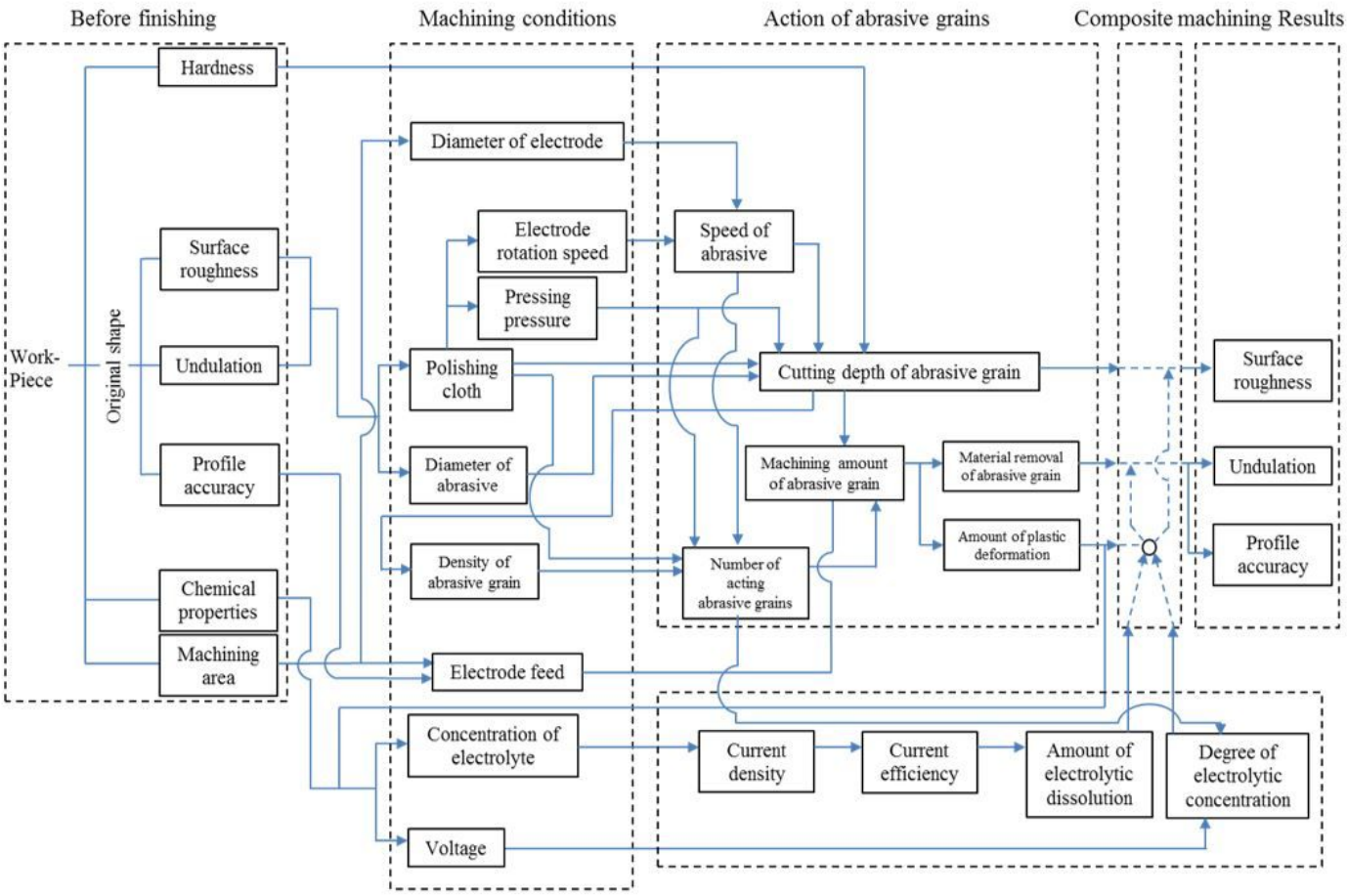

Figure 1

System model of electrochemical magnetic abrasive finishing

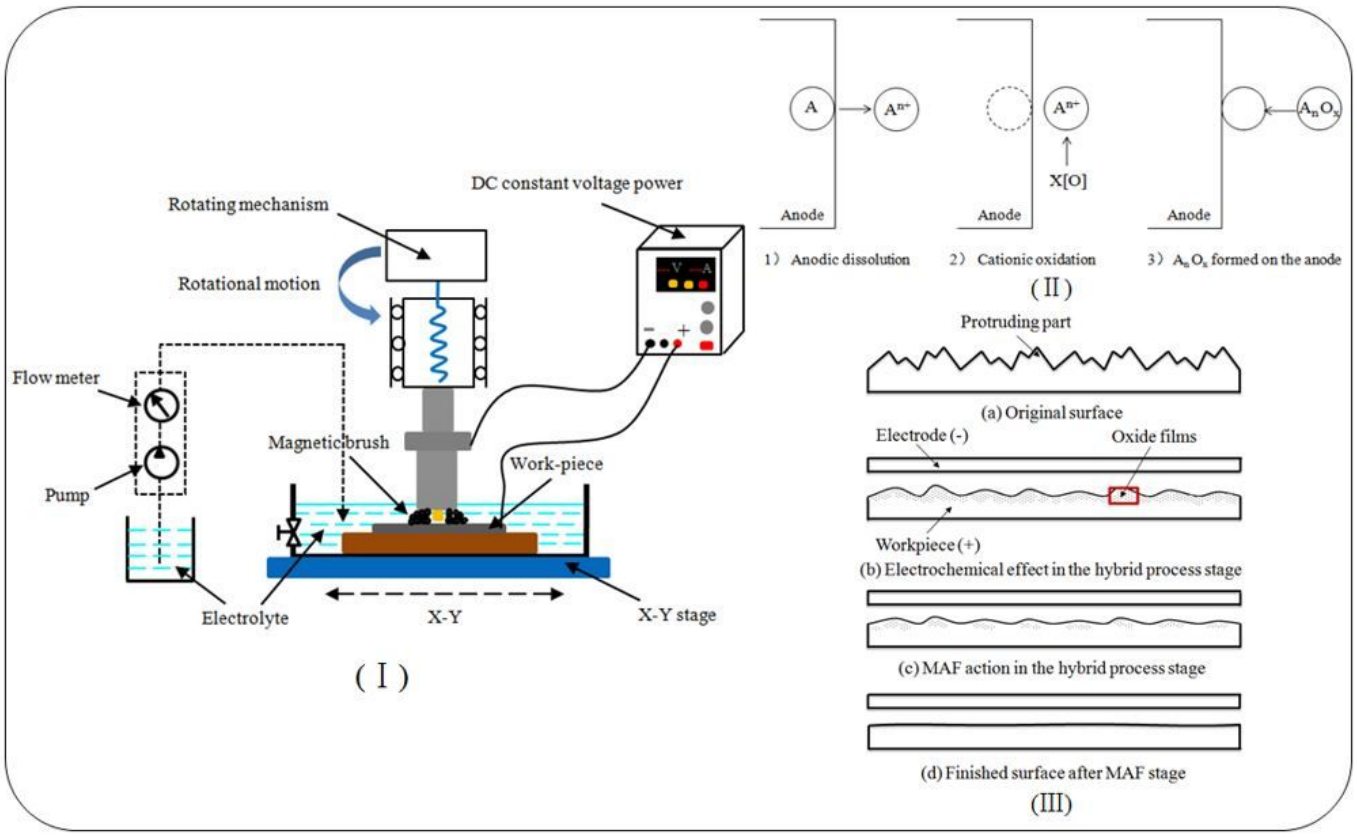

Figure 2

Schematic of EMAF process, (Ⅰ) the basic machining principle of EMAF process (Ⅱ) the forming mechanism of passive films in ECM process (Ⅲ) the whole process that the workpiece is finished by EMAF process

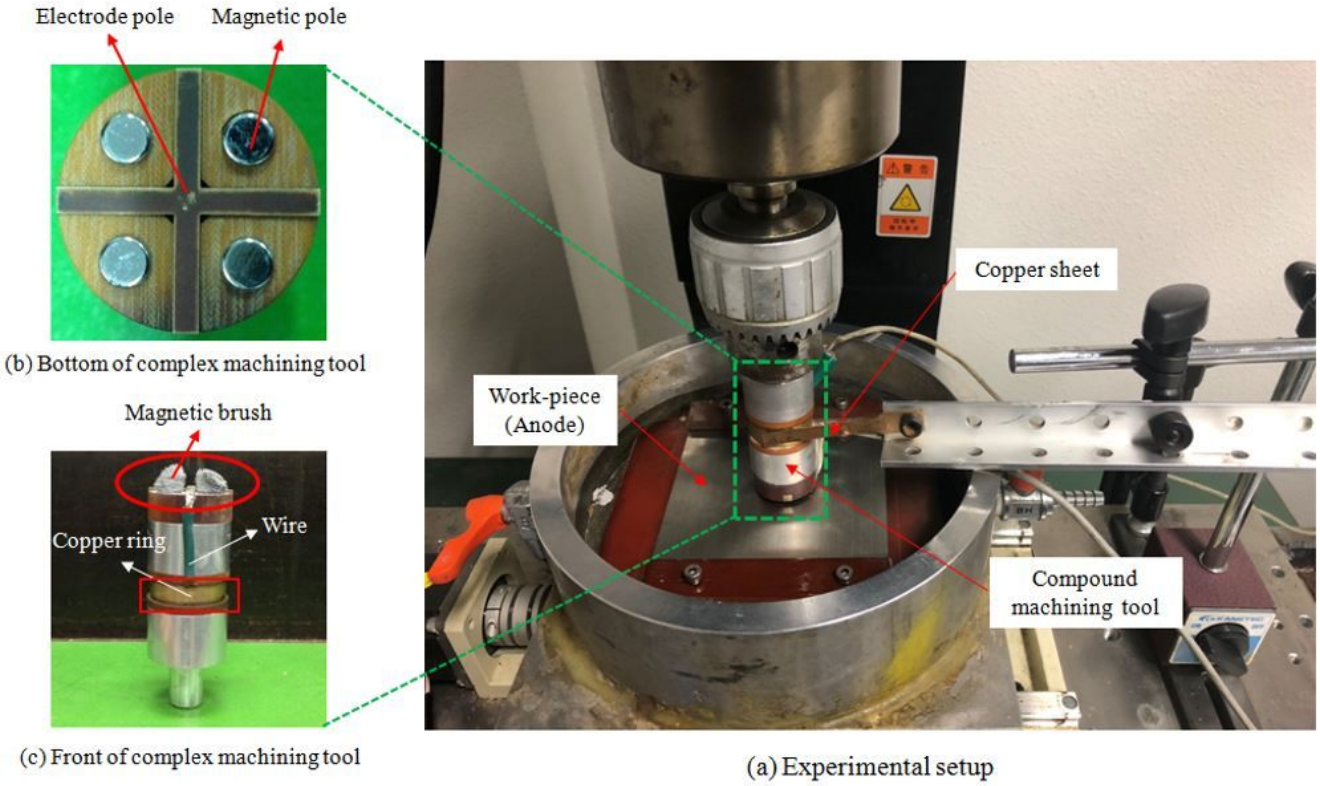

Figure 3

Photo of experimental setup and external views of electrochemical magnetic compound machining tool, (a) experimental setup (b) bottom of complex machining tool (c) front of complex machining tool

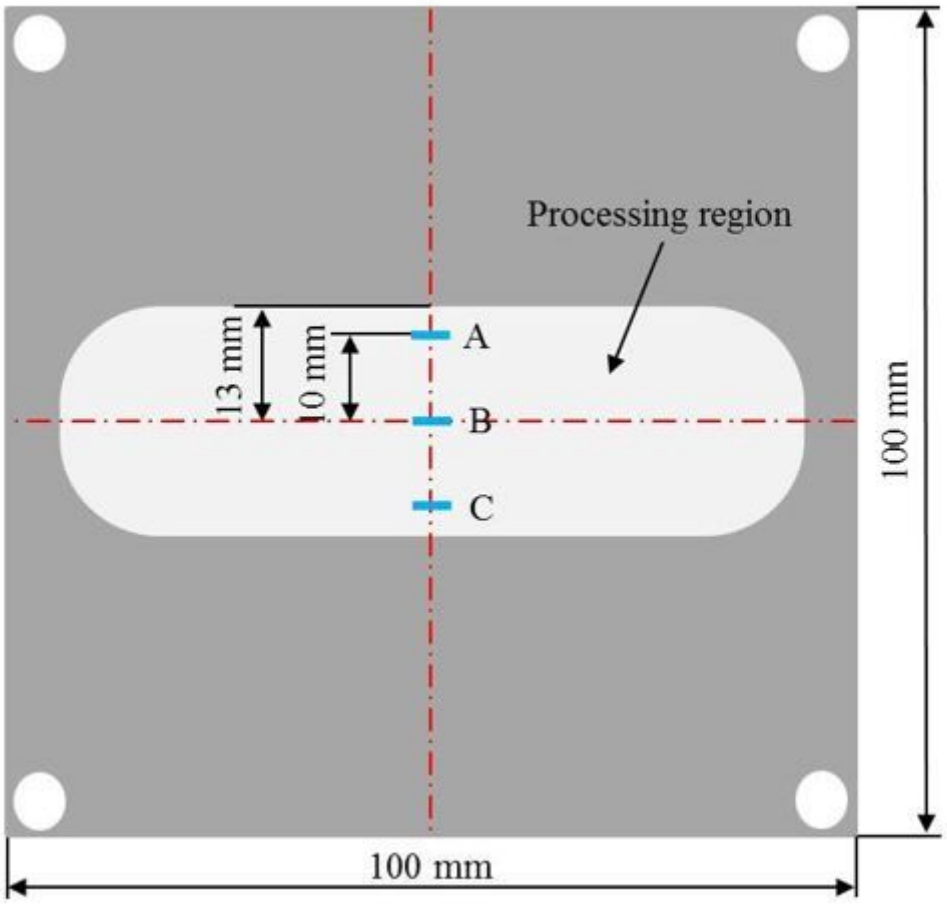

Figure 4

Observed locations of surface specimen

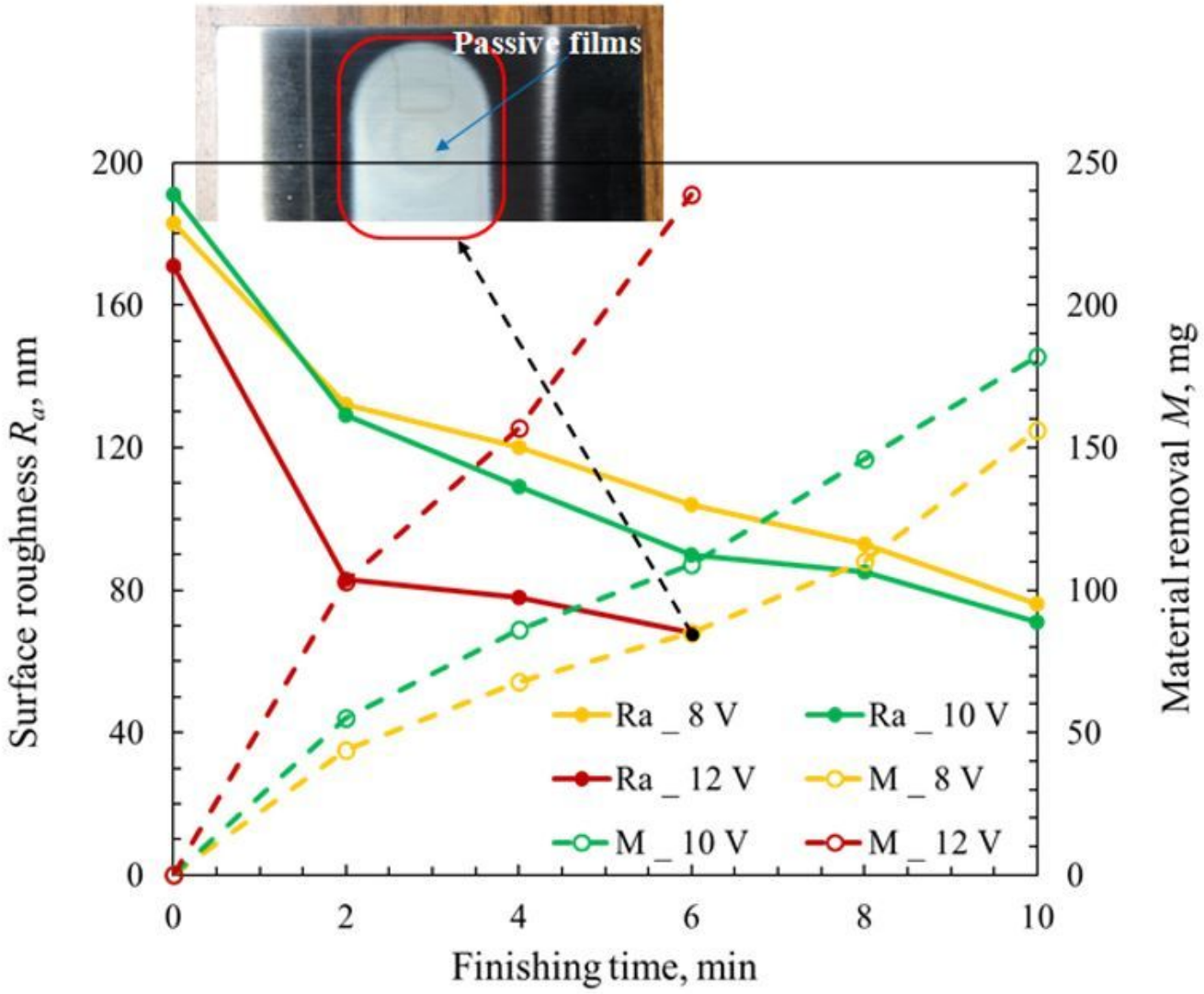

Figure 5

Change in surface roughness Ra and material removal M as a function of electrochemical machining time under various working voltage conditions

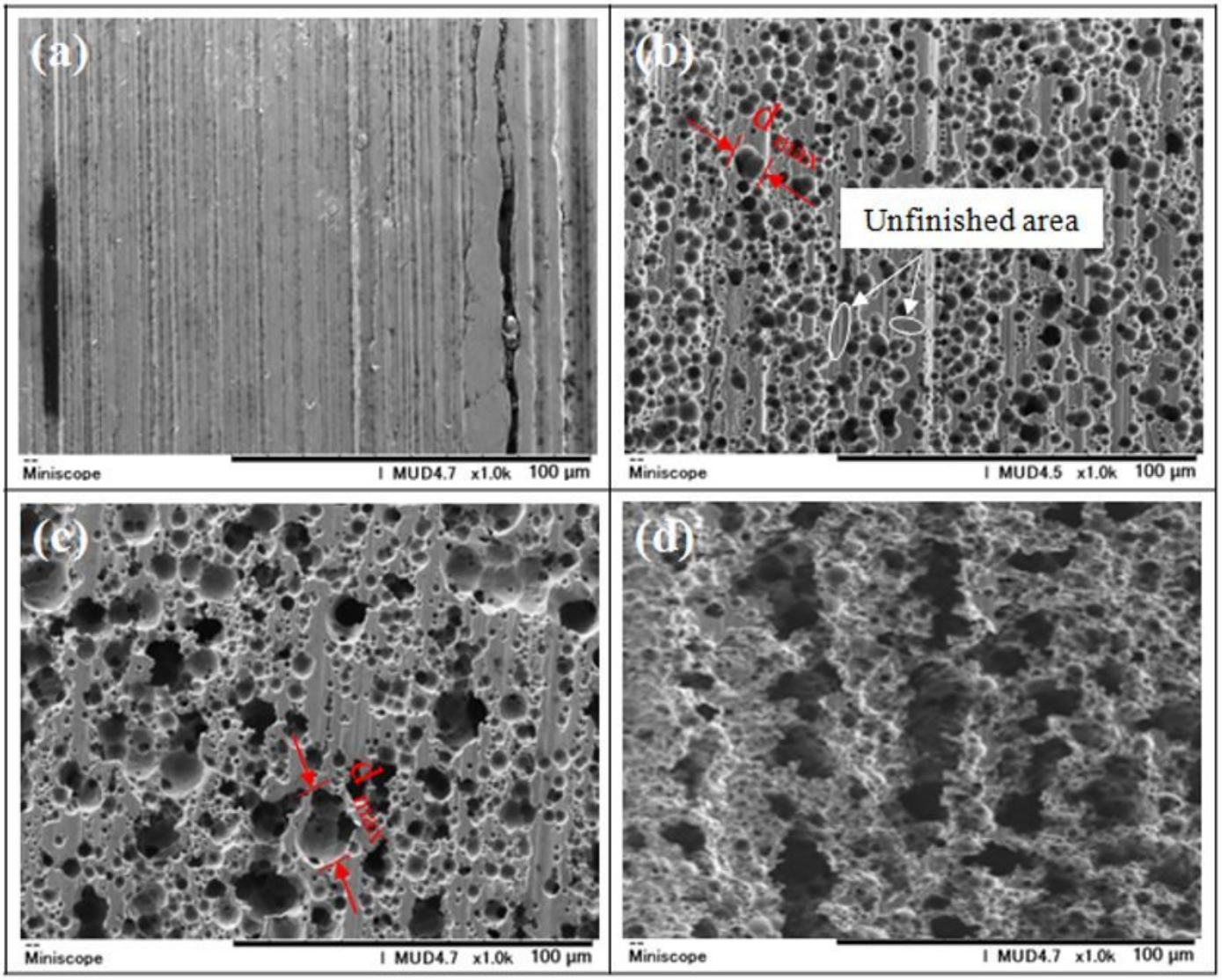

Figure 6

SEM images were obtained under different working voltage conditions in 4 min ECM process. (a) original workpiece surface; (b) under the condition of 8V working voltage; (c) under the condition of 10V working voltage; (c) under the condition of 12V working voltage.

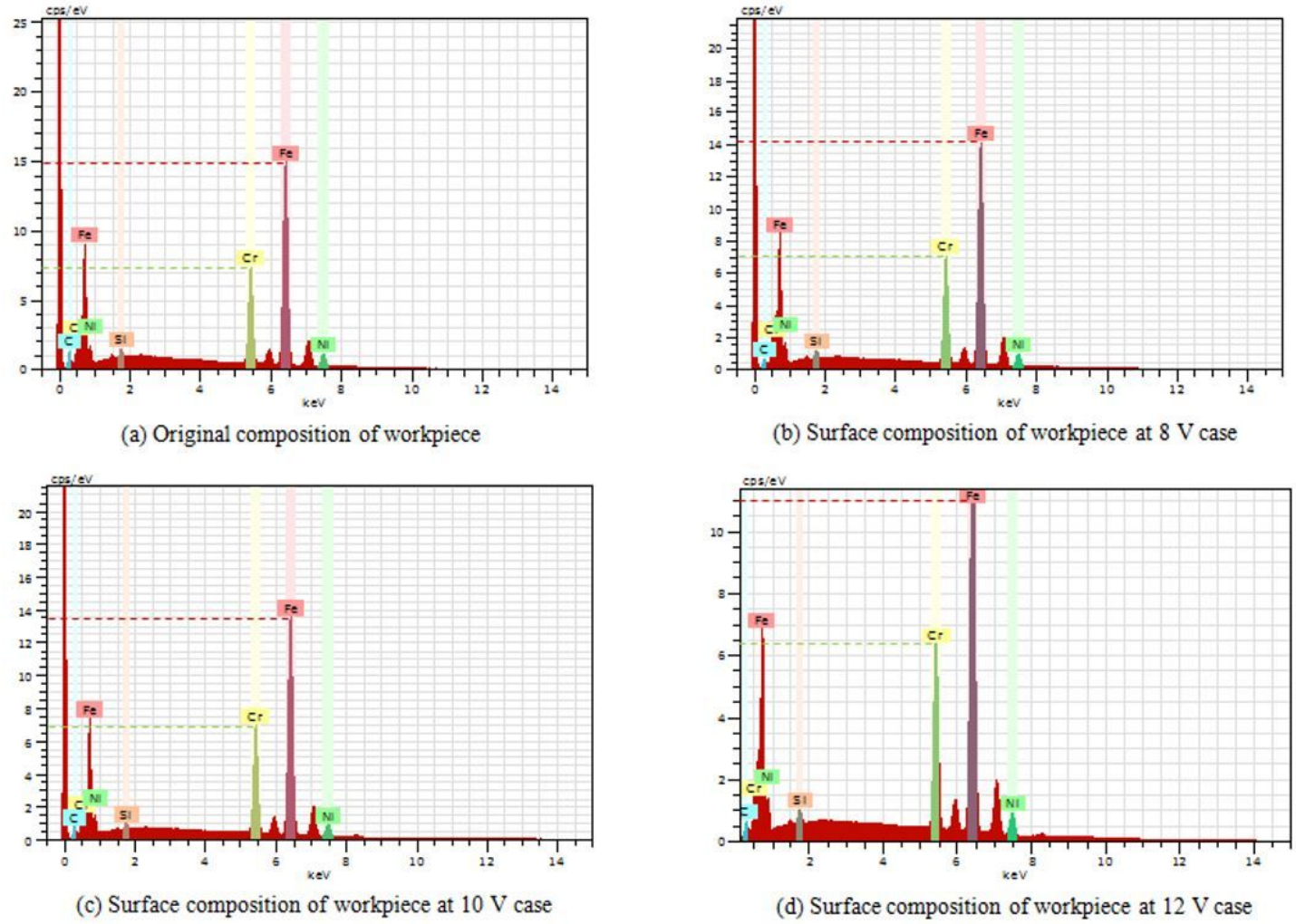

Figure 7

EDS of original surface and finished surface at different working voltage cases

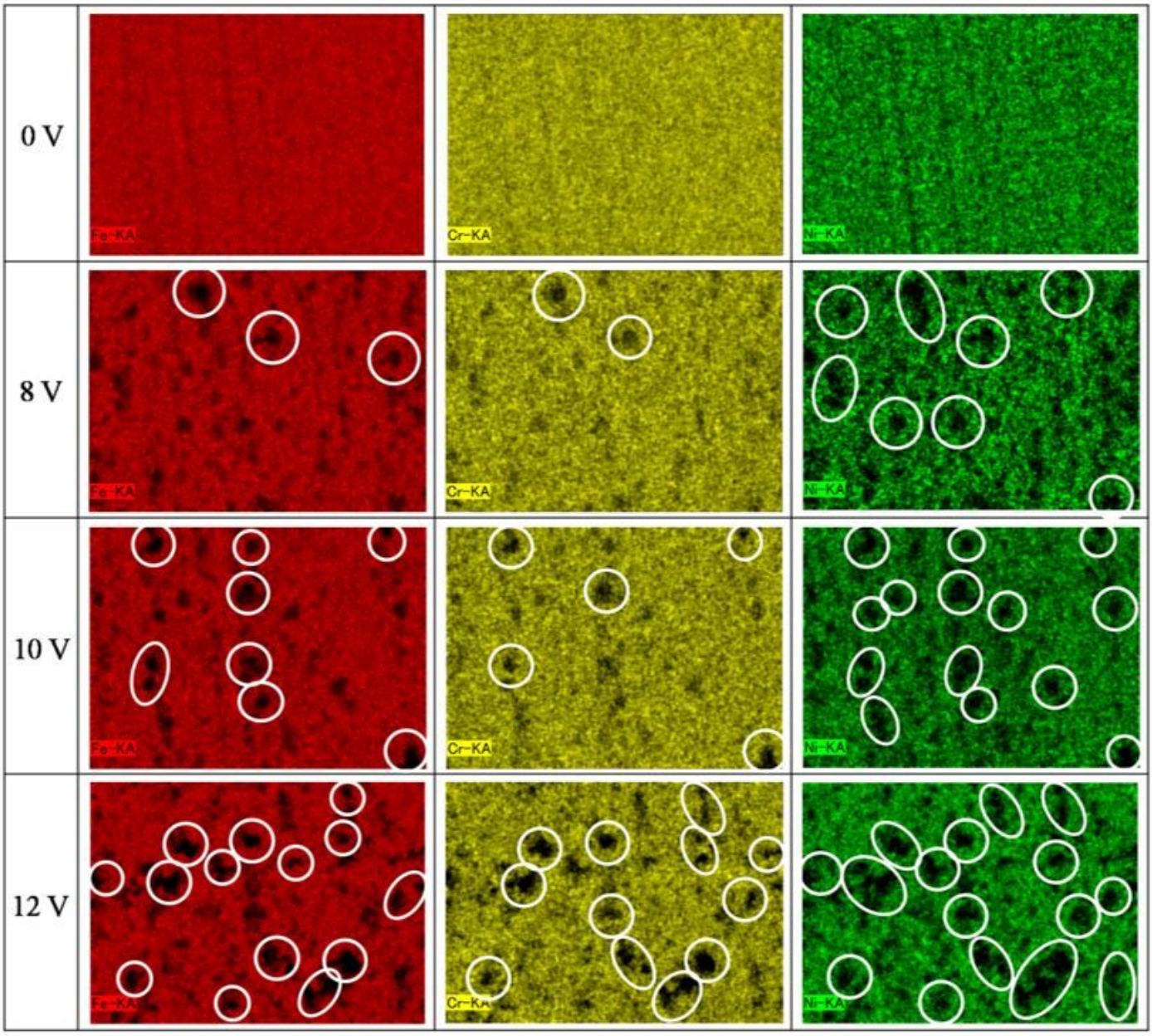

Figure 8

Chemical mapping of Fe, Cr and Ni elements after ECM process under various working voltage conditions

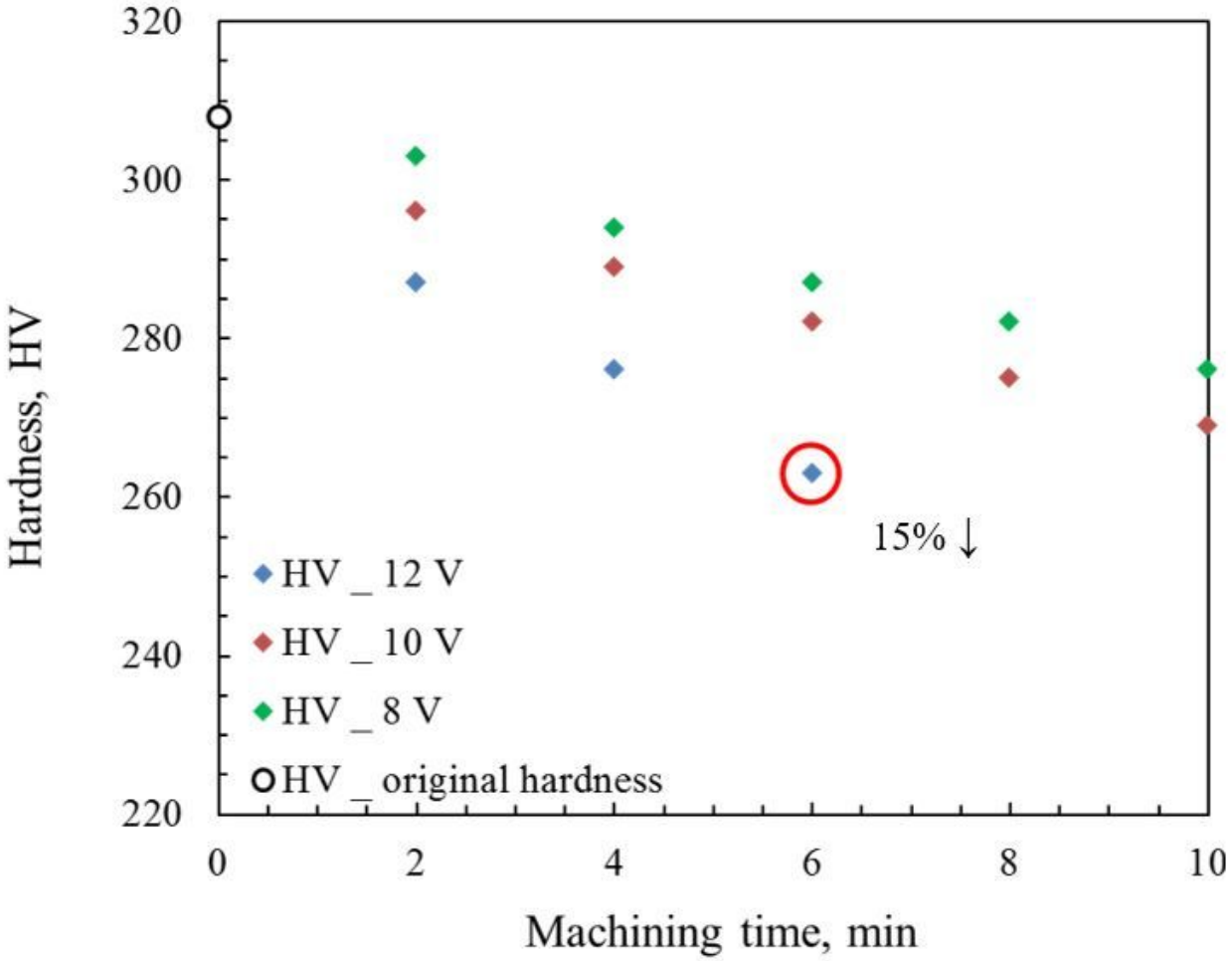

Figure 9

Change in hardness of workpiece surface under the electrochemical effect

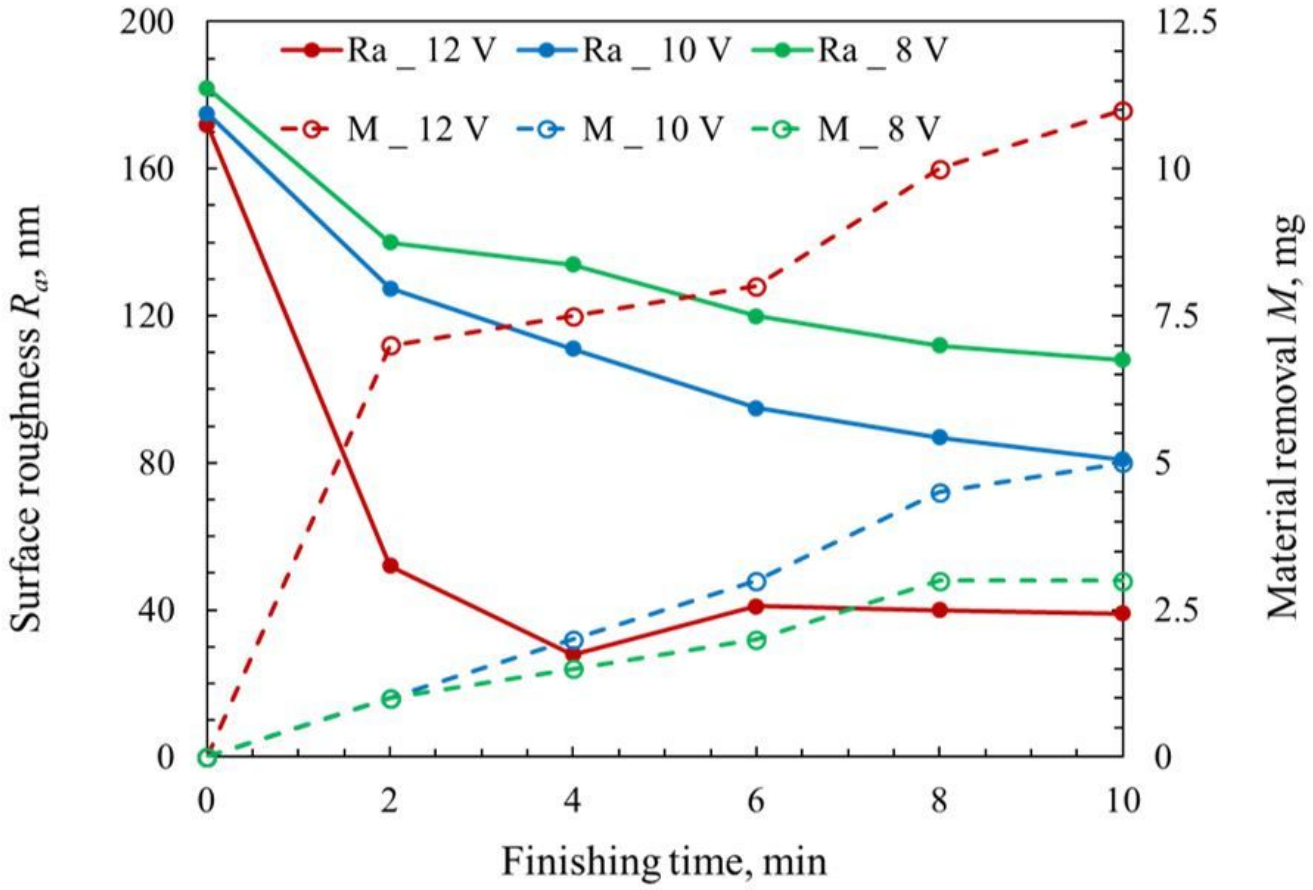

Figure 10

Change in surface roughness Ra and material removal M as a function under the conditions of different working voltage and finishing time

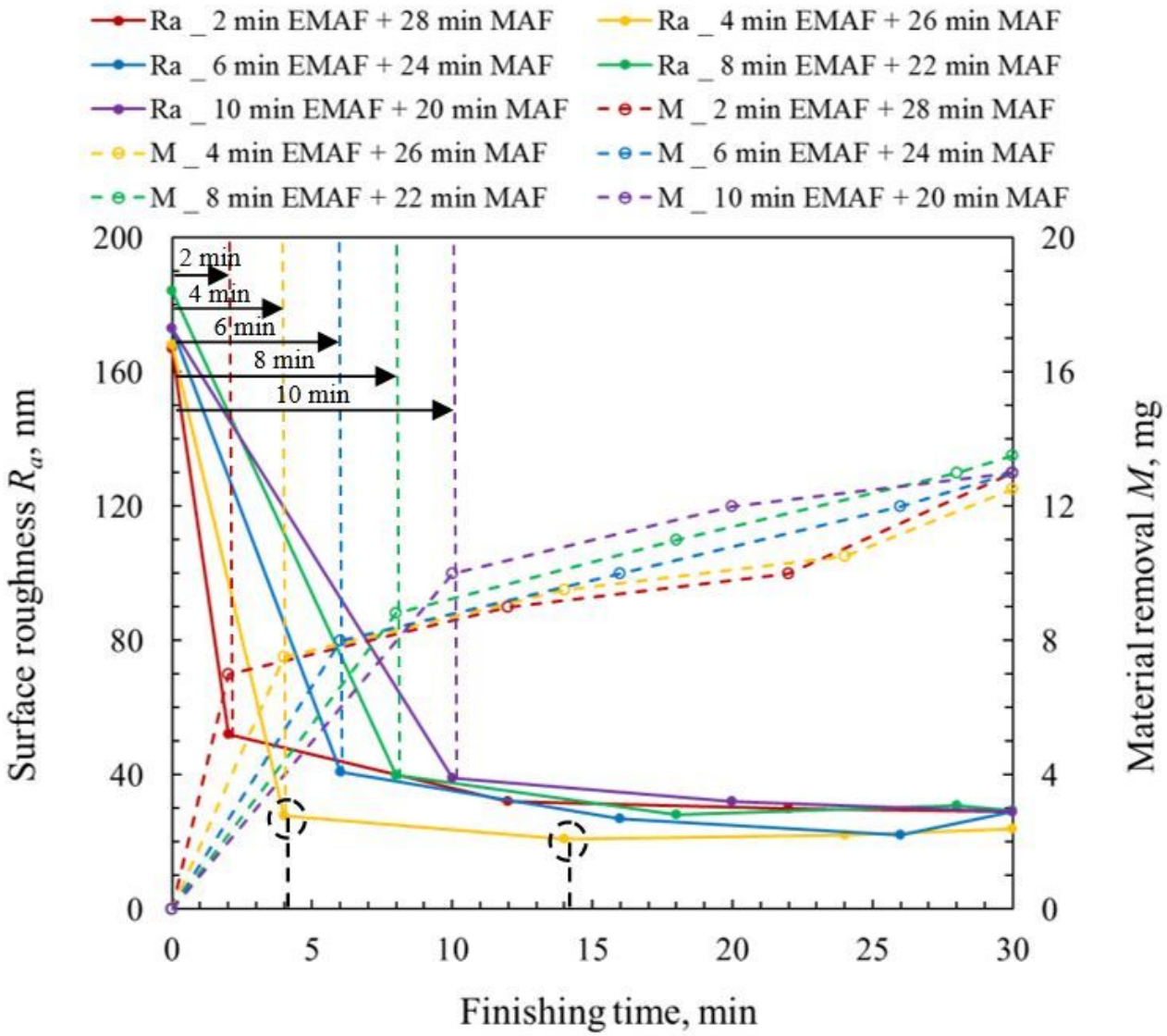

Figure 11

Change in surface roughness Ra and material removal M as a function under the different combination conditions of EMAF stage time and MAF stage time

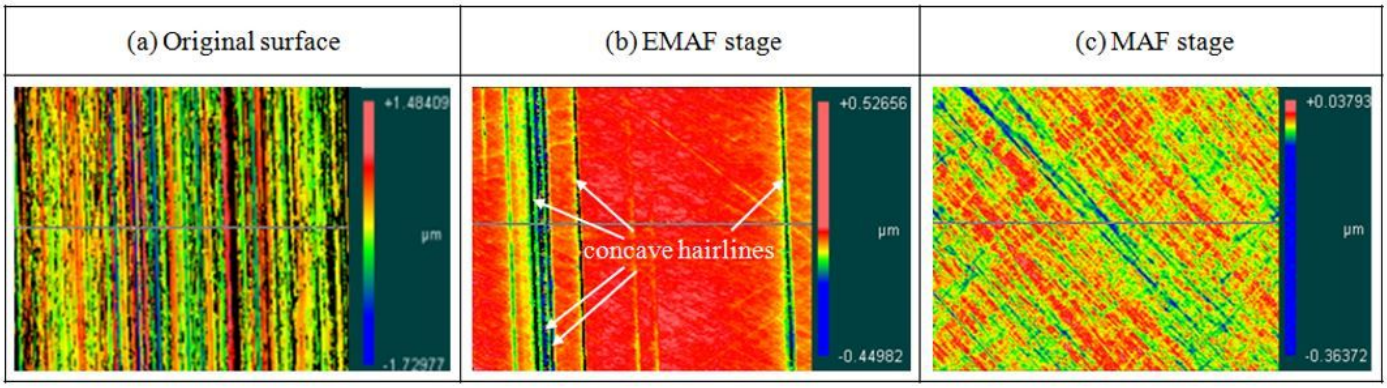

Figure 12

3D morphology of unfinished surface and finished surface after two different finishing stages

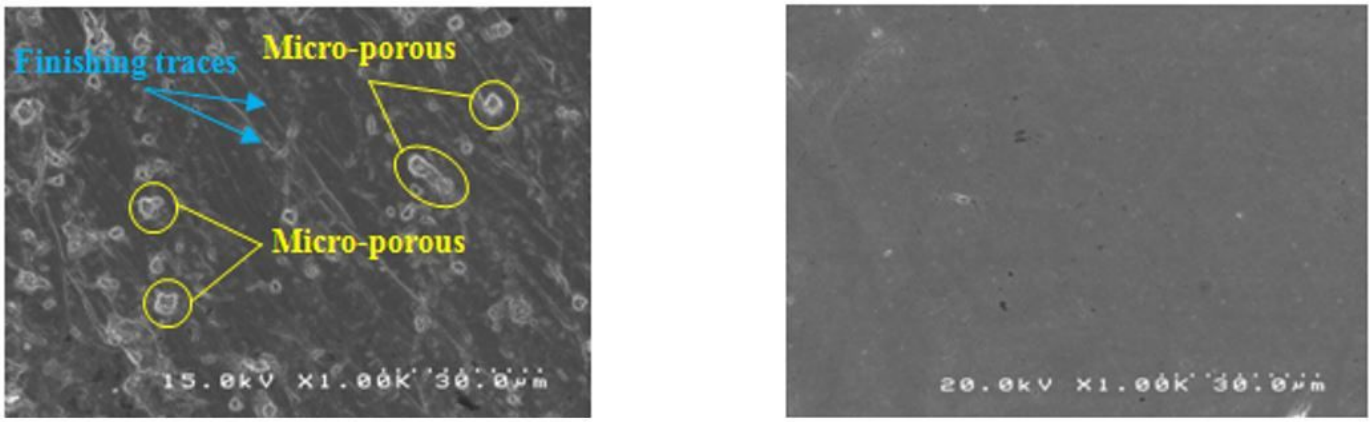

(a) After 4 min EMAF stage

(b) After 26 min MAF stage

Figure 13

Macroscopic confocal images of finished surface after EMAF stage and MAF stage

(a) Workpiece sample in ECM process (b) Workpiece sample in EMAF stage

Figure 14

The SUS304 workpiece was machined in ECM process and EMAF stage

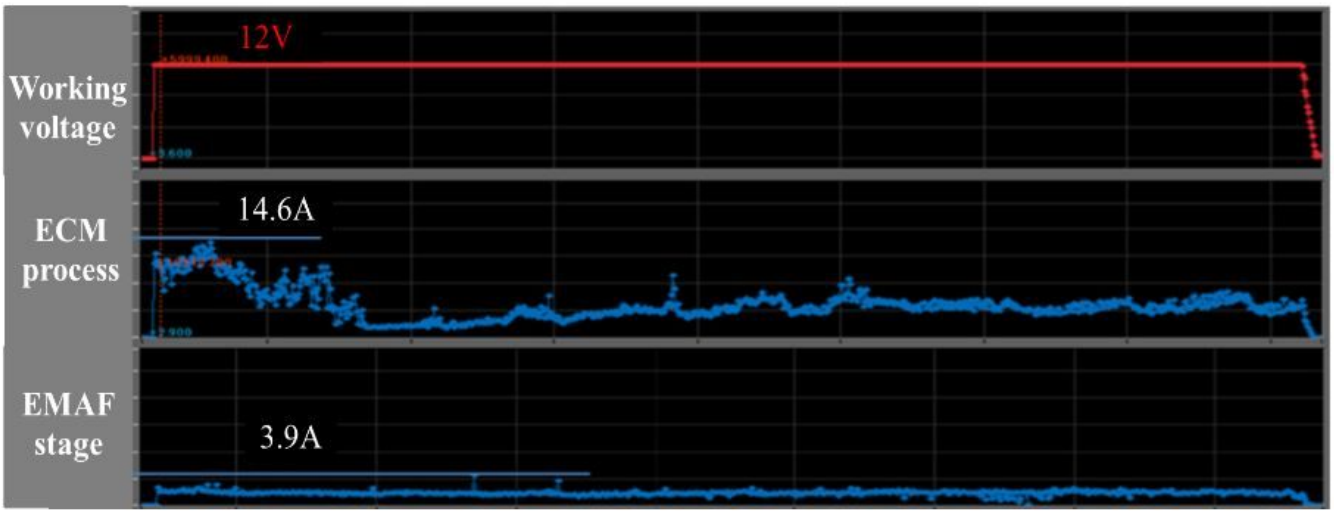

Figure 15

Electrolysis current in two different processing

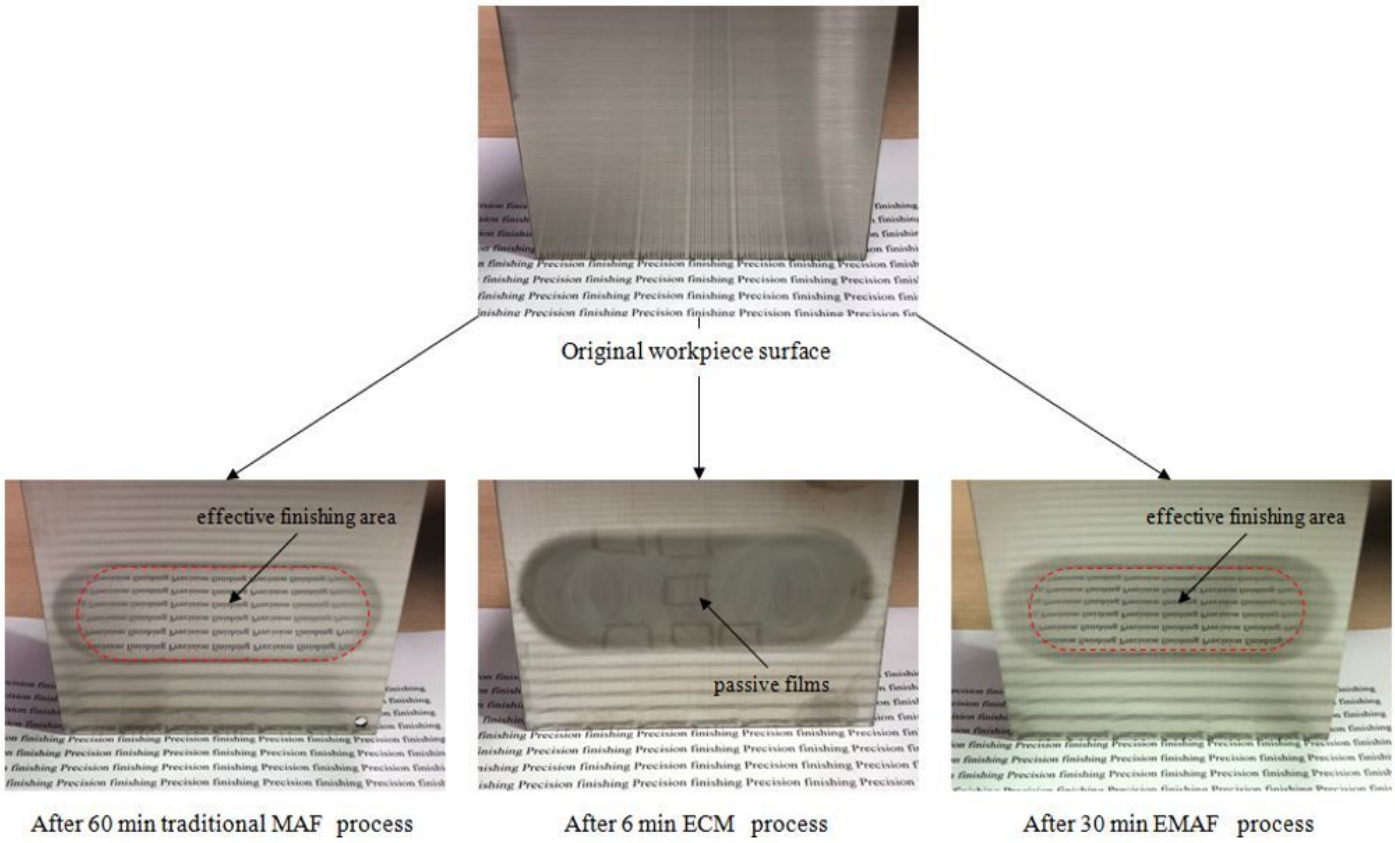

Figure 16

Photographs of unfinished surface and finished surface with three different finishing methods

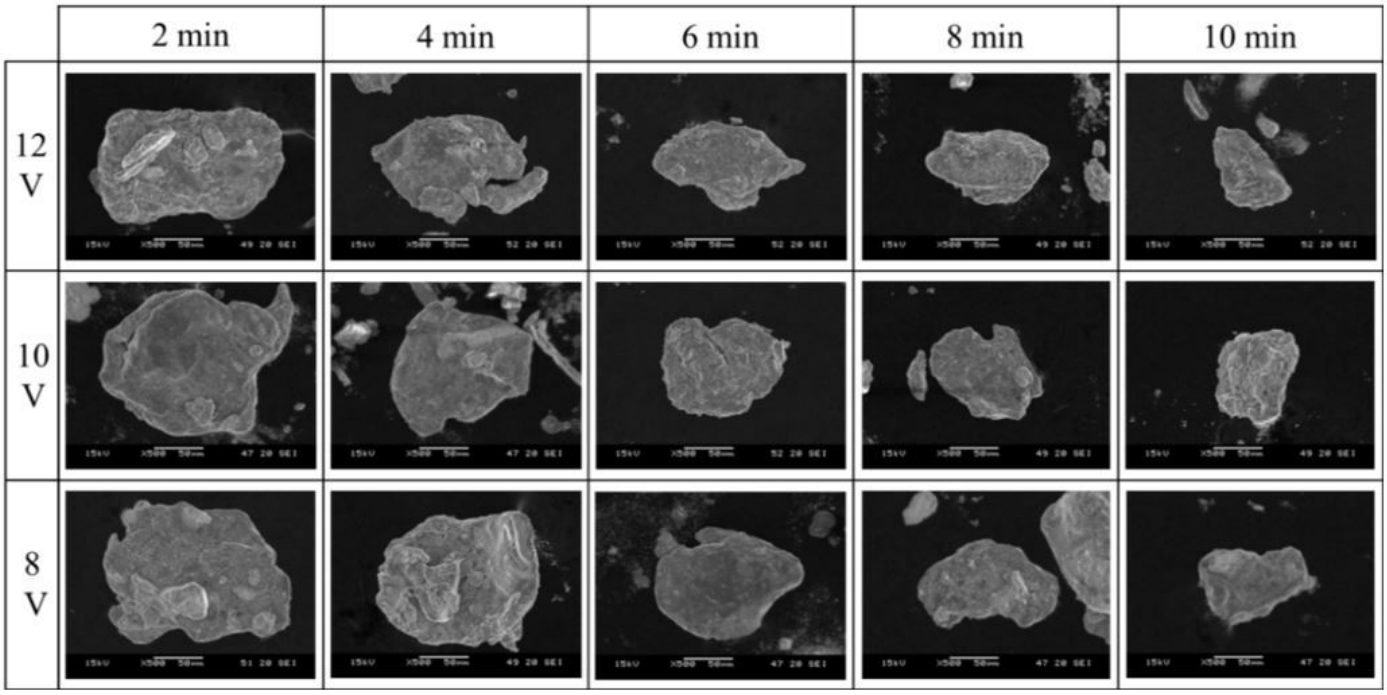

Figure 17

SEM images of change in mixed magnetic abrasive under the different conditions of EMAF stage time and working voltage